7

Dynamics

Derivation of the *dynamic model* of a manipulator plays an important role for simulation of motion, analysis of manipulator structures, and design of control algorithms. Simulating manipulator motion allows control strategies and motion planning techniques to be tested without the need to use a physically available system. The analysis of the dynamic model can be helpful for mechanical design of prototype arms. Computation of the forces and torques required for the execution of typical motions provides useful information for designing joints, transmissions and actuators. The goal of this chapter is to present two methods for derivation of the equations of motion of a manipulator in the *joint space*. The first method is based on the *Lagrange formulation* and is conceptually simple and systematic. The second method is based on the *Newton–Euler formulation* and yields the model in a recursive form; it is computationally more efficient since it exploits the typically open structure of the manipulator kinematic chain. Then, a technique for *dynamic parameter identification* is presented. Further, the problems of *direct dynamics* and *inverse dynamics* are formalized, and a technique for trajectory *dynamic scaling* is introduced, which adapts trajectory planning to the dynamic characteristics of the manipulator. The chapter ends with the derivation of the *dynamic model* of a manipulator in the *operational space* and the definition of the *dynamic manipulability ellipsoid*.

7.1 Lagrange Formulation

The dynamic model of a manipulator provides a description of the relationship between the joint actuator torques and the motion of the structure.

With *Lagrange formulation*, the equations of motion can be derived in a systematic way independently of the reference coordinate frame. Once a set of variables q_i, $i = 1, \ldots, n$, termed *generalized coordinates*, are chosen which effectively describe the link positions of an n-DOF manipulator, the

Lagrangian of the mechanical system can be defined as a function of the generalized coordinates:

$$\mathcal{L} = \mathcal{T} - \mathcal{U} \tag{7.1}$$

where T and U respectively denote the total *kinetic energy* and *potential energy* of the system.

The Lagrange equations are expressed by

$$\frac{d}{dt}\frac{\partial \mathcal{L}}{\partial \dot{q}_i} - \frac{\partial \mathcal{L}}{\partial q_i} = \xi_i \qquad i = 1, \ldots, n \tag{7.2}$$

where ξ_i is the *generalized force* associated with the generalized coordinate q_i. Equations (7.2) can be written in compact form as

$$\frac{d}{dt}\left(\frac{\partial \mathcal{L}}{\partial \dot{\boldsymbol{q}}}\right)^T - \left(\frac{\partial \mathcal{L}}{\partial \boldsymbol{q}}\right)^T = \boldsymbol{\xi} \tag{7.3}$$

where, for a manipulator with an open kinematic chain, the generalized coordinates are gathered in the vector of *joint variables* $\boldsymbol{q}$. The contributions to the generalized forces are given by the nonconservative forces, i.e., the joint actuator torques, the joint friction torques, as well as the joint torques induced by end-effector forces at the contact with the environment.[1]

The equations in (7.2) establish the relations existing between the generalized forces applied to the manipulator and the joint positions, velocities and accelerations. Hence, they allow the derivation of the dynamic model of the manipulator starting from the determination of kinetic energy and potential energy of the mechanical system.

Example 7.1

In order to understand the Lagrange formulation technique for deriving the dynamic model, consider again the simple case of the pendulum in Example 5.1. With reference to Fig. 5.8, let ϑ denote the angle with respect to the reference position of the body hanging down ($\vartheta = 0$). By choosing ϑ as the generalized coordinate, the kinetic energy of the system is given by

$$\mathcal{T} = \frac{1}{2} I \dot{\vartheta}^2 + \frac{1}{2} I_m k_r^2 \dot{\vartheta}^2.$$

The system potential energy, defined at less than a constant, is expressed by

$$\mathcal{U} = mg\ell(1 - \cos\vartheta).$$

Therefore, the Lagrangian of the system is

$$\mathcal{L} = \frac{1}{2} I \dot{\vartheta}^2 + \frac{1}{2} I_m k_r^2 \dot{\vartheta}^2 - mg\ell(1 - \cos\vartheta).$$

[1] The term *torque* is used as a synonym of joint *generalized force*.

Substituting this expression in the Lagrange equation in (7.2) yields

$$(I + I_m k_r^2)\ddot{\vartheta} + mg\ell \sin \vartheta = \xi.$$

The generalized force ξ is given by the contributions of the actuation torque τ at the joint and of the viscous friction torques $-F\dot{\vartheta}$ and $-F_m k_r^2 \dot{\vartheta}$, where the latter has been reported to the joint side. Hence, it is

$$\xi = \tau - F\dot{\vartheta} - F_m k_r^2 \dot{\vartheta}$$

leading to the complete dynamic model of the system as the second-order differential equation

$$(I + I_m k_r^2)\ddot{\vartheta} + (F + F_m k_r^2)\dot{\vartheta} + mg\ell \sin \vartheta = \tau.$$

It is easy to verify how this equation is equivalent to (5.29) when reported to the joint side.

7.1.1 Computation of Kinetic Energy

Consider a manipulator with n *rigid links*. The total kinetic energy is given by the sum of the contributions relative to the motion of each link and the contributions relative to the motion of each joint actuator:[2]

$$\mathcal{T} = \sum_{i=1}^{n} (\mathcal{T}_{\ell_i} + \mathcal{T}_{m_i}), \tag{7.4}$$

where $\mathcal{T}_{\ell_i}$ is the kinetic energy of Link i and $\mathcal{T}_{m_i}$ is the kinetic energy of the motor actuating Joint i.

The kinetic energy contribution of Link i is given by

$$\mathcal{T}_{\ell_i} = \frac{1}{2} \int_{V_{\ell_i}} \dot{\boldsymbol{p}}_i^{*T} \dot{\boldsymbol{p}}_i^{*} \rho dV, \tag{7.5}$$

where $\dot{\boldsymbol{p}}_i^*$ denotes the linear velocity vector and ρ is the density of the elementary particle of volume dV; V_{ℓ_i} is the volume of Link i.

Consider the position vector $\boldsymbol{p}_i^*$ of the elementary particle and the position vector $\boldsymbol{p}_{C_i}$ of the link centre of mass, both expressed in the *base frame*. One has

$$\boldsymbol{r}_i = [\, r_{ix} \quad r_{iy} \quad r_{iz} \,]^T = \boldsymbol{p}_i^* - \boldsymbol{p}_{\ell_i} \tag{7.6}$$

with

$$\boldsymbol{p}_{\ell_i} = \frac{1}{m_{\ell_i}} \int_{V_{\ell_i}} \boldsymbol{p}_i^* \rho dV \tag{7.7}$$

---

[2] Link 0 is fixed and thus gives no contribution.

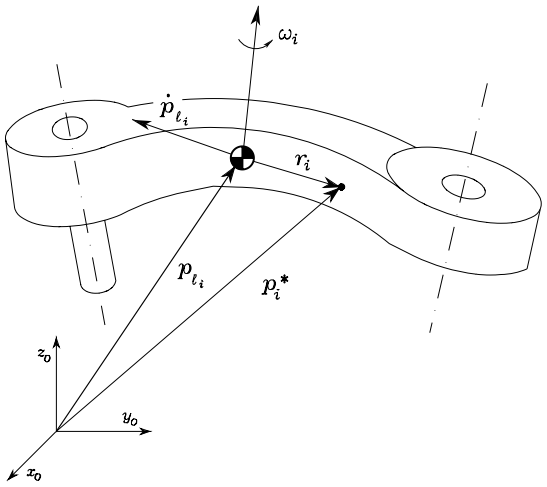

Fig. 7.1. Kinematic description of Link i for Lagrange formulation

where m_{ℓ_i} is the link mass. As a consequence, the link point velocity can be expressed as

$$\begin{aligned} \dot{\boldsymbol{p}}_i^* &= \dot{\boldsymbol{p}}_{\ell_i} + \boldsymbol{\omega}_i \times \boldsymbol{r}_i \\ &= \dot{\boldsymbol{p}}_{\ell_i} + \boldsymbol{S}(\boldsymbol{\omega}_i)\boldsymbol{r}_i, \end{aligned} \tag{7.8}$$

where $\dot{\boldsymbol{p}}_{\ell_i}$ is the linear velocity of the centre of mass and $\boldsymbol{\omega}_i$ is the angular velocity of the link (Fig. 7.1).

By substituting the velocity expression (7.8) into (7.5), it can be recognized that the kinetic energy of each link is formed by the following contributions.

Translational

The contribution is

$$\frac{1}{2}\int_{V_{\ell_i}} \dot{\boldsymbol{p}}_{\ell_i}^T \dot{\boldsymbol{p}}_{\ell_i} \rho dV = \frac{1}{2} m_{\ell_i} \dot{\boldsymbol{p}}_{\ell_i}^T \dot{\boldsymbol{p}}_{\ell_i}. \tag{7.9}$$

Mutual

The contribution is

$$2\left(\frac{1}{2}\int_{V_{\ell_i}} \dot{\boldsymbol{p}}_{\ell_i}^T \boldsymbol{S}(\boldsymbol{\omega}_i)\boldsymbol{r}_i \rho dV\right) = 2\left(\frac{1}{2}\dot{\boldsymbol{p}}_{\ell_i}^T \boldsymbol{S}(\boldsymbol{\omega}_i)\int_{V_{\ell_i}} (\boldsymbol{p}_i^* - \boldsymbol{p}_{\ell_i})\rho dV\right) = 0$$

since, by virtue of (7.7), it is

$$\int_{V_{\ell_i}} \boldsymbol{p}_i^* \rho dV = \boldsymbol{p}_{\ell_i} \int_{V_{\ell_i}} \rho dV.$$

Rotational

The contribution is

$$\frac{1}{2}\int_{V_{\ell_i}} \boldsymbol{r}_i^T \boldsymbol{S}^T(\boldsymbol{\omega}_i)\boldsymbol{S}(\boldsymbol{\omega}_i)\boldsymbol{r}_i \rho dV = \frac{1}{2}\boldsymbol{\omega}_i^T \left(\int_{V_{\ell_i}} \boldsymbol{S}^T(\boldsymbol{r}_i)\boldsymbol{S}(\boldsymbol{r}_i)\rho dV\right)\boldsymbol{\omega}_i$$

where the property $\boldsymbol{S}(\boldsymbol{\omega}_i)\boldsymbol{r}_i = -\boldsymbol{S}(\boldsymbol{r}_i)\boldsymbol{\omega}_i$ has been exploited. In view of the expression of the matrix operator $\boldsymbol{S}(\cdot)$

$$\boldsymbol{S}(\boldsymbol{r}_i) = \begin{bmatrix} 0 & -r_{iz} & r_{iy} \\ r_{iz} & 0 & -r_{ix} \\ -r_{iy} & r_{ix} & 0 \end{bmatrix},$$

it is

$$\frac{1}{2}\int_{V_{\ell_i}} \boldsymbol{r}_i^T \boldsymbol{S}^T(\boldsymbol{\omega}_i)\boldsymbol{S}(\boldsymbol{\omega}_i)\boldsymbol{r}_i \rho dV = \frac{1}{2}\boldsymbol{\omega}_i^T \boldsymbol{I}_{\ell_i}\boldsymbol{\omega}_i. \tag{7.10}$$

The matrix

$$\begin{aligned} \boldsymbol{I}_{\ell_i} &= \begin{bmatrix} \int(r_{iy}^2 + r_{iz}^2)\rho dV & -\int r_{ix}r_{iy}\rho dV & -\int r_{ix}r_{iz}\rho dV \\ * & \int(r_{ix}^2 + r_{iz}^2)\rho dV & -\int r_{iy}r_{iz}\rho dV \\ * & * & \int(r_{ix}^2 + r_{iy}^2)\rho dV \end{bmatrix} \\ &= \begin{bmatrix} I_{\ell_i xx} & -I_{\ell_i xy} & -I_{\ell_i xz} \\ * & I_{\ell_i yy} & -I_{\ell_i yz} \\ * & * & I_{\ell_i zz} \end{bmatrix}. \end{aligned} \tag{7.11}$$

is symmetric[3] and represents the *inertia tensor* relative to the centre of mass of Link i when expressed in the base frame. Notice that the position of Link i depends on the manipulator configuration and thus the inertia tensor, when expressed in the base frame, is configuration-dependent. If the angular velocity of Link i is expressed with reference to a frame attached to the link (as in the Denavit–Hartenberg convention), it is

$$\boldsymbol{\omega}_i^i = \boldsymbol{R}_i^T \boldsymbol{\omega}_i$$

where $\boldsymbol{R}_i$ is the rotation matrix from Link i frame to the base frame. When referred to the link frame, the inertia tensor is constant. Let $\boldsymbol{I}_{\ell_i}^i$ denote such tensor; then it is easy to verify the following relation:

$$\boldsymbol{I}_{\ell_i} = \boldsymbol{R}_i \boldsymbol{I}_{\ell_i}^i \boldsymbol{R}_i^T. \tag{7.12}$$

If the axes of Link i frame coincide with the central axes of inertia, then the inertia products are null and the inertia tensor relative to the centre of mass is a diagonal matrix.

[3] The symbol '$*$' has been used to avoid rewriting the symmetric elements.

By summing the translational and rotational contributions (7.9) and (7.10), the kinetic energy of Link i is

$$\mathcal{T}_{\ell_i} = \frac{1}{2} m_{\ell_i} \dot{\boldsymbol{p}}_{\ell_i}^T \dot{\boldsymbol{p}}_{\ell_i} + \frac{1}{2} \boldsymbol{\omega}_i^T \boldsymbol{R}_i \boldsymbol{I}_{\ell_i}^i \boldsymbol{R}_i^T \boldsymbol{\omega}_i. \tag{7.13}$$

At this point, it is necessary to express the kinetic energy as a function of the generalized coordinates of the system, that are the joint variables. To this end, the geometric method for Jacobian computation can be applied to the intermediate link other than the end-effector, yielding

$$\dot{\boldsymbol{p}}_{\ell_i} = \boldsymbol{\jmath}_{P1}^{(\ell_i)} \dot{q}_1 + \ldots + \boldsymbol{\jmath}_{Pi}^{(\ell_i)} \dot{q}_i = \boldsymbol{J}_P^{(\ell_i)} \dot{\boldsymbol{q}} \tag{7.14}$$

$$\boldsymbol{\omega}_i = \boldsymbol{\jmath}_{O1}^{(\ell_i)} \dot{q}_1 + \ldots + \boldsymbol{\jmath}_{Oi}^{(\ell_i)} \dot{q}_i = \boldsymbol{J}_O^{(\ell_i)} \dot{\boldsymbol{q}}, \tag{7.15}$$

where the contributions of the Jacobian columns relative to the joint velocities have been taken into account up to current Link i. The Jacobians to consider are then:

$$\boldsymbol{J}_P^{(\ell_i)} = \begin{bmatrix} \boldsymbol{\jmath}_{P1}^{(\ell_i)} & \ldots & \boldsymbol{\jmath}_{Pi}^{(\ell_i)} & \boldsymbol{0} & \ldots & \boldsymbol{0} \end{bmatrix} \tag{7.16}$$

$$\boldsymbol{J}_O^{(\ell_i)} = \begin{bmatrix} \boldsymbol{\jmath}_{O1}^{(\ell_i)} & \ldots & \boldsymbol{\jmath}_{Oi}^{(\ell_i)} & \boldsymbol{0} & \ldots & \boldsymbol{0} \end{bmatrix}; \tag{7.17}$$

the columns of the matrices in (7.16) and (7.17) can be computed according to (3.30), giving

$$\boldsymbol{\jmath}_{Pj}^{(\ell_i)} = \begin{cases} \boldsymbol{z}_{j-1} & \text{for a } \textit{prismatic} \text{ joint} \\ \boldsymbol{z}_{j-1} \times (\boldsymbol{p}_{\ell_i} - \boldsymbol{p}_{j-1}) & \text{for a } \textit{revolute} \text{ joint} \end{cases} \tag{7.18}$$

$$\boldsymbol{\jmath}_{Oj}^{(\ell_i)} = \begin{cases} \boldsymbol{0} & \text{for a } \textit{prismatic} \text{ joint} \\ \boldsymbol{z}_{j-1} & \text{for a } \textit{revolute} \text{ joint.} \end{cases} \tag{7.19}$$

where $\boldsymbol{p}_{j-1}$ is the position vector of the origin of Frame $j-1$ and $\boldsymbol{z}_{j-1}$ is the unit vector of axis z of Frame $j-1$. It follows that the kinetic energy of Link i in (7.13) can be written as

$$\mathcal{T}_{\ell_i} = \frac{1}{2} m_{\ell_i} \dot{\boldsymbol{q}}^T \boldsymbol{J}_P^{(\ell_i)T} \boldsymbol{J}_P^{(\ell_i)} \dot{\boldsymbol{q}} + \frac{1}{2} \dot{\boldsymbol{q}}^T \boldsymbol{J}_O^{(\ell_i)T} \boldsymbol{R}_i \boldsymbol{I}_{\ell_i}^i \boldsymbol{R}_i^T \boldsymbol{J}_O^{(\ell_i)} \dot{\boldsymbol{q}}. \tag{7.20}$$

The kinetic energy contribution of the motor of Joint i can be computed in a formally analogous way to that of the link. Consider the typical case of rotary electric motors (that can actuate both revolute and prismatic joints by means of suitable transmissions). It can be assumed that the contribution of the fixed part (stator) is included in that of the link on which such motor is located, and thus the sole contribution of the rotor is to be computed.

With reference to Fig. 7.2, the motor of Joint i is assumed to be located on Link $i-1$. In practice, in the design of the mechanical structure of an open kinematic chain manipulator one attempts to locate the motors as close as possible to the base of the manipulator so as to lighten the dynamic load of

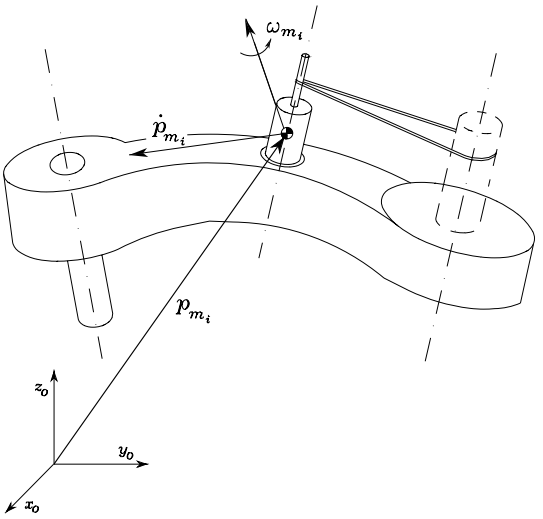

Fig. 7.2. Kinematic description of Motor i

the first joints of the chain. The joint actuator torques are delivered by the motors by means of mechanical transmissions (gears).[4] The contribution of the gears to the kinetic energy can be suitably included in that of the motor. It is assumed that no induced motion occurs, i.e., the motion of Joint i does not actuate the motion of other joints.

The kinetic energy of Rotor i can be written as

$$\mathcal{T}_{m_i} = \frac{1}{2} m_{m_i} \dot{\boldsymbol{p}}_{m_i}^T \dot{\boldsymbol{p}}_{m_i} + \frac{1}{2} \boldsymbol{\omega}_{m_i}^T \boldsymbol{I}_{m_i} \boldsymbol{\omega}_{m_i}, \tag{7.21}$$

where m_{m_i} is the mass of the rotor, $\dot{\boldsymbol{p}}_{m_i}$ denotes the linear velocity of the centre of mass of the rotor, $\boldsymbol{I}_{m_i}$ is the inertia tensor of the rotor relative to its centre of mass, and $\boldsymbol{\omega}_{m_i}$ denotes the angular velocity of the rotor.

Let ϑ_{m_i} denote the angular position of the rotor. On the assumption of a *rigid transmission*, one has

$$k_{ri} \dot{q}_i = \dot{\vartheta}_{m_i} \tag{7.22}$$

where k_{ri} is the gear reduction ratio. Notice that, in the case of actuation of a prismatic joint, the gear reduction ratio is a dimensional quantity.

According to the angular velocity composition rule (3.18) and the relation (7.22), the total angular velocity of the rotor is

$$\boldsymbol{\omega}_{m_i} = \boldsymbol{\omega}_{i-1} + k_{ri} \dot{q}_i \boldsymbol{z}_{m_i} \tag{7.23}$$

where $\boldsymbol{\omega}_{i-1}$ is the angular velocity of Link $i-1$ on which the motor is located, and $\boldsymbol{z}_{m_i}$ denotes the unit vector along the rotor axis.

[4] Alternatively, the joints may be actuated by torque motors directly coupled to the rotation axis without gears.

To express the rotor kinetic energy as a function of the joint variables, it is worth expressing the linear velocity of the rotor centre of mass — similarly to (7.14) — as

$$\dot{\boldsymbol{p}}_{m_i} = \boldsymbol{J}_P^{(m_i)} \dot{\boldsymbol{q}}. \tag{7.24}$$

The Jacobian to compute is then

$$\boldsymbol{J}_P^{(m_i)} = \begin{bmatrix} \boldsymbol{\jmath}_{P1}^{(m_i)} & \cdots & \boldsymbol{\jmath}_{P,i-1}^{(m_i)} & \boldsymbol{0} & \cdots & \boldsymbol{0} \end{bmatrix} \tag{7.25}$$

whose columns are given by

$$\boldsymbol{\jmath}_{Pj}^{(m_i)} = \begin{cases} \boldsymbol{z}_{j-1} & \text{for a } \textit{prismatic} \text{ joint} \\ \boldsymbol{z}_{j-1} \times (\boldsymbol{p}_{m_i} - \boldsymbol{p}_{j-1}) & \text{for a } \textit{revolute} \text{ joint} \end{cases} \tag{7.26}$$

where $\boldsymbol{p}_{j-1}$ is the position vector of the origin of Frame $j-1$. Notice that $\boldsymbol{\jmath}_{Pi}^{(m_i)} = \boldsymbol{0}$ in (7.25), since the centre of mass of the rotor has been taken along its axis of rotation.

The angular velocity in (7.23) can be expressed as a function of the joint variables, i.e.,

$$\boldsymbol{\omega}_{m_i} = \boldsymbol{J}_O^{(m_i)} \dot{\boldsymbol{q}}. \tag{7.27}$$

The Jacobian to compute is then

$$\boldsymbol{J}_O^{(m_i)} = \begin{bmatrix} \boldsymbol{\jmath}_{O1}^{(m_i)} & \cdots & \boldsymbol{\jmath}_{O,i-1}^{(m_i)} & \boldsymbol{\jmath}_{Oi}^{(m_i)} & \boldsymbol{0} & \cdots & \boldsymbol{0} \end{bmatrix} \tag{7.28}$$

whose columns, in view of (7.23), (7.15), are respectively given by

$$\boldsymbol{\jmath}_{Oj}^{(m_i)} = \begin{cases} \boldsymbol{\jmath}_{Oj}^{(\ell_i)} & j = 1, \ldots, i-1 \\ k_{ri} \boldsymbol{z}_{m_i} & j = i. \end{cases} \tag{7.29}$$

To compute the second relation in (7.29), it is sufficient to know the components of the unit vector of the rotor rotation axis $\boldsymbol{z}_{m_i}$ with respect to the base frame. Hence, the kinetic energy of Rotor i can be written as

$$\mathcal{T}_{m_i} = \frac{1}{2} m_{m_i} \dot{\boldsymbol{q}}^T \boldsymbol{J}_P^{(m_i)T} \boldsymbol{J}_P^{(m_i)} \dot{\boldsymbol{q}} + \frac{1}{2} \dot{\boldsymbol{q}}^T \boldsymbol{J}_O^{(m_i)T} \boldsymbol{R}_{m_i} \boldsymbol{I}_{m_i}^{m_i} \boldsymbol{R}_{m_i}^T \boldsymbol{J}_O^{(m_i)} \dot{\boldsymbol{q}}. \tag{7.30}$$

Finally, by summing the various contributions relative to the single links (7.20) and single rotors (7.30) as in (7.4), the total kinetic energy of the manipulator with actuators is given by the quadratic form

$$\mathcal{T} = \frac{1}{2} \sum_{i=1}^{n} \sum_{j=1}^{n} b_{ij}(\boldsymbol{q}) \dot{q}_i \dot{q}_j = \frac{1}{2} \dot{\boldsymbol{q}}^T \boldsymbol{B}(\boldsymbol{q}) \dot{\boldsymbol{q}} \tag{7.31}$$

where

$$\begin{aligned} \boldsymbol{B}(\boldsymbol{q}) = \sum_{i=1}^{n} \Big(& m_{\ell_i} \boldsymbol{J}_P^{(\ell_i)T} \boldsymbol{J}_P^{(\ell_i)} + \boldsymbol{J}_O^{(\ell_i)T} \boldsymbol{R}_i \boldsymbol{I}_{\ell_i}^i \boldsymbol{R}_i^T \boldsymbol{J}_O^{(\ell_i)} \\ & + m_{m_i} \boldsymbol{J}_P^{(m_i)T} \boldsymbol{J}_P^{(m_i)} + \boldsymbol{J}_O^{(m_i)T} \boldsymbol{R}_{m_i} \boldsymbol{I}_{m_i}^{m_i} \boldsymbol{R}_{m_i}^T \boldsymbol{J}_O^{(m_i)} \Big) \end{aligned} \tag{7.32}$$

is the $(n \times n)$ *inertia matrix* which is:

- *symmetric*,
- *positive definite*,
- (in general) *configuration-dependent*.

7.1.2 Computation of Potential Energy

As done for kinetic energy, the potential energy stored in the manipulator is given by the sum of the contributions relative to each link as well as to each rotor:

$$\mathcal{U} = \sum_{i=1}^{n} (\mathcal{U}_{\ell_i} + \mathcal{U}_{m_i}). \tag{7.33}$$

On the assumption of *rigid links*, the contribution due only to gravitational forces[5] is expressed by

$$\mathcal{U}_{\ell_i} = -\int_{V_{\ell_i}} \boldsymbol{g}_0^T \boldsymbol{p}_i^* \rho dV = -m_{\ell_i} \boldsymbol{g}_0^T \boldsymbol{p}_{\ell_i} \tag{7.34}$$

where $\boldsymbol{g}_0$ is the gravity acceleration vector in the base frame (e.g., $\boldsymbol{g}_0 = [\,0 \quad 0 \quad -g\,]^T$ if z is the vertical axis), and (7.7) has been utilized for the coordinates of the centre of mass of Link i. As regards the contribution of Rotor i, similarly to (7.34), one has

$$\mathcal{U}_{m_i} = -m_{m_i} \boldsymbol{g}_0^T \boldsymbol{p}_{m_i}. \tag{7.35}$$

By substituting (7.34), (7.35) into (7.33), the *potential energy* is given by

$$\mathcal{U} = -\sum_{i=1}^{n} (m_{\ell_i} \boldsymbol{g}_0^T \boldsymbol{p}_{\ell_i} + m_{m_i} \boldsymbol{g}_0^T \boldsymbol{p}_{m_i}) \tag{7.36}$$

which reveals that potential energy, through the vectors $\boldsymbol{p}_{\ell_i}$ and $\boldsymbol{p}_{m_i}$ is a function only of the joint variables $\boldsymbol{q}$, and *not* of the joint velocities $\dot{\boldsymbol{q}}$.

7.1.3 Equations of Motion

Having computed the total kinetic and potential energy of the system as in (7.31), (7.36), the Lagrangian (7.1) for the manipulator can be written as

$$\mathcal{L}(\boldsymbol{q}, \dot{\boldsymbol{q}}) = \mathcal{T}(\boldsymbol{q}, \dot{\boldsymbol{q}}) - \mathcal{U}(\boldsymbol{q}). \tag{7.37}$$

Taking the derivatives required by Lagrange equations in (7.3) and recalling that U does not depend on $\dot{\boldsymbol{q}}$ yields

$$\boldsymbol{B}(\boldsymbol{q})\ddot{\boldsymbol{q}} + \boldsymbol{n}(\boldsymbol{q}, \dot{\boldsymbol{q}}) = \boldsymbol{\xi} \tag{7.38}$$

[5] In the case of link flexibility, one would have an additional contribution due to elastic forces.

where

$$\boldsymbol{n}(\boldsymbol{q},\dot{\boldsymbol{q}}) = \dot{\boldsymbol{B}}(\boldsymbol{q})\dot{\boldsymbol{q}} - \frac{1}{2}\left(\frac{\partial}{\partial \boldsymbol{q}}\left(\dot{\boldsymbol{q}}^T\boldsymbol{B}(\boldsymbol{q})\dot{\boldsymbol{q}}\right)\right)^T + \left(\frac{\partial \mathcal{U}(\boldsymbol{q})}{\partial \boldsymbol{q}}\right)^T.$$

In detail, noticing that $\mathcal{U}$ in (7.36) does not depend on $\dot{\boldsymbol{q}}$ and accounting for (7.31) yields

$$\begin{aligned}\frac{d}{dt}\left(\frac{\partial \mathcal{L}}{\partial \dot{q}_i}\right) = \frac{d}{dt}\left(\frac{\partial \mathcal{T}}{\partial \dot{q}_i}\right) &= \sum_{j=1}^{n} b_{ij}(\boldsymbol{q})\ddot{q}_j + \sum_{j=1}^{n}\frac{db_{ij}(\boldsymbol{q})}{dt}\dot{q}_j \\ &= \sum_{j=1}^{n} b_{ij}(\boldsymbol{q})\ddot{q}_j + \sum_{j=1}^{n}\sum_{k=1}^{n}\frac{\partial b_{ij}(\boldsymbol{q})}{\partial q_k}\dot{q}_k\dot{q}_j\end{aligned}$$

and

$$\frac{\partial \mathcal{T}}{\partial q_i} = \frac{1}{2}\sum_{j=1}^{n}\sum_{k=1}^{n}\frac{\partial b_{jk}(\boldsymbol{q})}{\partial q_i}\dot{q}_k\dot{q}_j$$

where the indices of summation have been conveniently switched. Further, in view of (7.14), (7.24), it is

$$\begin{aligned}\frac{\partial \mathcal{U}}{\partial q_i} &= -\sum_{j=1}^{n}\left(m_{\ell_j}\boldsymbol{g}_0^T\frac{\partial \boldsymbol{p}_{\ell_j}}{\partial q_i} + m_{m_j}\boldsymbol{g}_0^T\frac{\partial \boldsymbol{p}_{m_j}}{\partial q_i}\right) \qquad (7.39)\\ &= -\sum_{j=1}^{n}\left(m_{\ell_j}\boldsymbol{g}_0^T\boldsymbol{\jmath}_{Pi}^{(\ell_j)}(\boldsymbol{q}) + m_{m_j}\boldsymbol{g}_0^T\boldsymbol{\jmath}_{Pi}^{(m_j)}(\boldsymbol{q})\right) = g_i(\boldsymbol{q})\end{aligned}$$

where, again, the index of summation has been changed.

As a result, the equations of motion are

$$\sum_{j=1}^{n} b_{ij}(\boldsymbol{q})\ddot{q}_j + \sum_{j=1}^{n}\sum_{k=1}^{n} h_{ijk}(\boldsymbol{q})\dot{q}_k\dot{q}_j + g_i(\boldsymbol{q}) = \xi_i \qquad i = 1,\dots,n \qquad (7.40)$$

where

$$h_{ijk} = \frac{\partial b_{ij}}{\partial q_k} - \frac{1}{2}\frac{\partial b_{jk}}{\partial q_i}. \qquad (7.41)$$

A physical interpretation of (7.40) reveals that:

- For the *acceleration terms*:
  - The coefficient b_{ii} represents the moment of inertia at Joint i axis, in the current manipulator configuration, when the other joints are blocked.
  - The coefficient b_{ij} accounts for the effect of acceleration of Joint j on Joint j.
- For the *quadratic velocity terms*:
  - The term $h_{ijj}\dot{q}_j^2$ represents the *centrifugal* effect induced on Joint i by velocity of Joint j; notice that $h_{iii} = 0$, since $\partial b_{ii}/\partial q_i = 0$.

  - The term $h_{ijk}\dot{q}_j\dot{q}_k$ represents the *Coriolis* effect induced on Joint i by velocities of Joints j and k.
- For the *configuration-dependent terms*:
  - The term g_i represents the moment generated at Joint i axis of the manipulator, in the current configuration, by the presence of gravity.

Some joint dynamic couplings, e.g., coefficients b_{ij} and h_{ijk}, may be reduced or zeroed when designing the structure, so as to simplify the control problem.

Regarding the nonconservative forces doing work at the manipulator joints, these are given by the *actuation torques* $\boldsymbol{\tau}$ minus the *viscous friction* torques $\boldsymbol{F}_v\dot{\boldsymbol{q}}$ and the static friction torques $\boldsymbol{f}_s(\boldsymbol{q},\dot{\boldsymbol{q}})$: $\boldsymbol{F}_v$ denotes the $(n \times n)$ diagonal matrix of viscous friction coefficients. As a simplified model of static friction torques, one may consider the *Coulomb friction* torques $\boldsymbol{F}_s\,\mathbf{sgn}\,(\dot{\boldsymbol{q}})$, where $\boldsymbol{F}_s$ is an $(n \times n)$ diagonal matrix and $\mathbf{sgn}\,(\dot{\boldsymbol{q}})$ denotes the $(n \times 1)$ vector whose components are given by the sign functions of the single joint velocities.

If the manipulator's end-effector is in contact with an environment, a portion of the actuation torques is used to balance the torques induced at the joints by the contact forces. According to a relation formally analogous to (3.111), such torques are given by $\boldsymbol{J}^T(\boldsymbol{q})\boldsymbol{h}_e$ where $\boldsymbol{h}_e$ denotes the vector of force and moment exerted by the end-effector on the environment.

In summary, the equations of motion (7.38) can be rewritten in the compact matrix form which represents the *joint space dynamic model*:

$$\boldsymbol{B}(\boldsymbol{q})\ddot{\boldsymbol{q}} + \boldsymbol{C}(\boldsymbol{q},\dot{\boldsymbol{q}})\dot{\boldsymbol{q}} + \boldsymbol{F}_v\dot{\boldsymbol{q}} + \boldsymbol{F}_s\,\mathbf{sgn}\,(\dot{\boldsymbol{q}}) + \boldsymbol{g}(\boldsymbol{q}) = \boldsymbol{\tau} - \boldsymbol{J}^T(\boldsymbol{q})\boldsymbol{h}_e \tag{7.42}$$

where $\boldsymbol{C}$ is a suitable $(n \times n)$ matrix such that its elements c_{ij} satisfy the equation

$$\sum_{j=1}^{n} c_{ij}\dot{q}_j = \sum_{j=1}^{n}\sum_{k=1}^{n} h_{ijk}\dot{q}_k\dot{q}_j. \tag{7.43}$$

7.2 Notable Properties of Dynamic Model

In the following, two *notable properties* of the dynamic model are presented which will be useful for dynamic parameter identification as well as for deriving control algorithms.

7.2.1 Skew-symmetry of Matrix $\dot{\boldsymbol{B}} - 2\boldsymbol{C}$

The choice of the matrix $\boldsymbol{C}$ is not unique, since there exist several matrices $\boldsymbol{C}$ whose elements satisfy (7.43). A particular choice can be obtained by

elaborating the term on the right-hand side of (7.43) and accounting for the expressions of the coefficients h_{ijk} in (7.41). To this end, one has

$$\begin{aligned}\sum_{j=1}^{n} c_{ij}\dot{q}_j &= \sum_{j=1}^{n}\sum_{k=1}^{n} h_{ijk}\dot{q}_k\dot{q}_j \\ &= \sum_{j=1}^{n}\sum_{k=1}^{n}\left(\frac{\partial b_{ij}}{\partial q_k} - \frac{1}{2}\frac{\partial b_{jk}}{\partial q_i}\right)\dot{q}_k\dot{q}_j.\end{aligned}$$

Splitting the first term on the right-hand side by an opportune switch of summation between j and k yields

$$\sum_{j=1}^{n} c_{ij}\dot{q}_j = \frac{1}{2}\sum_{j=1}^{n}\sum_{k=1}^{n}\frac{\partial b_{ij}}{\partial q_k}\dot{q}_k\dot{q}_j + \frac{1}{2}\sum_{j=1}^{n}\sum_{k=1}^{n}\left(\frac{\partial b_{ik}}{\partial q_j} - \frac{\partial b_{jk}}{\partial q_i}\right)\dot{q}_k\dot{q}_j.$$

As a consequence, the generic element of $\boldsymbol{C}$ is

$$c_{ij} = \sum_{k=1}^{n} c_{ijk}\dot{q}_k \tag{7.44}$$

where the coefficients

$$c_{ijk} = \frac{1}{2}\left(\frac{\partial b_{ij}}{\partial q_k} + \frac{\partial b_{ik}}{\partial q_j} - \frac{\partial b_{jk}}{\partial q_i}\right) \tag{7.45}$$

are termed *Christoffel symbols of the first type*. Notice that, in view of the symmetry of $\boldsymbol{B}$, it is

$$c_{ijk} = c_{ikj}. \tag{7.46}$$

This choice for the matrix $\boldsymbol{C}$ leads to deriving the following notable property of the equations of motion (7.42). The matrix

$$\boldsymbol{N}(\boldsymbol{q}, \dot{\boldsymbol{q}}) = \dot{\boldsymbol{B}}(\boldsymbol{q}) - 2\boldsymbol{C}(\boldsymbol{q}, \dot{\boldsymbol{q}}) \tag{7.47}$$

is *skew-symmetric*; that is, given any $(n \times 1)$ vector $\boldsymbol{w}$, the following relation holds:

$$\boldsymbol{w}^T\boldsymbol{N}(\boldsymbol{q}, \dot{\boldsymbol{q}})\boldsymbol{w} = 0. \tag{7.48}$$

In fact, substituting the coefficient (7.45) into (7.44) gives

$$\begin{aligned}c_{ij} &= \frac{1}{2}\sum_{k=1}^{n}\frac{\partial b_{ij}}{\partial q_k}\dot{q}_k + \frac{1}{2}\sum_{k=1}^{n}\left(\frac{\partial b_{ik}}{\partial q_j} - \frac{\partial b_{jk}}{\partial q_i}\right)\dot{q}_k \\ &= \frac{1}{2}\dot{b}_{ij} + \frac{1}{2}\sum_{k=1}^{n}\left(\frac{\partial b_{ik}}{\partial q_j} - \frac{\partial b_{jk}}{\partial q_i}\right)\dot{q}_k\end{aligned}$$

and then the expression of the generic element of the matrix $\boldsymbol{N}$ in (7.47) is

$$n_{ij} = \dot{b}_{ij} - 2c_{ij} = \sum_{k=1}^{n}\left(\frac{\partial b_{jk}}{\partial q_i} - \frac{\partial b_{ik}}{\partial q_j}\right)\dot{q}_k.$$

The result follows by observing that

$$n_{ij} = -n_{ji}.$$

An interesting property which is a direct implication of the skew-symmetry of $\boldsymbol{N}(\boldsymbol{q}, \dot{\boldsymbol{q}})$ is that, by setting $\boldsymbol{w} = \dot{\boldsymbol{q}}$,

$$\dot{\boldsymbol{q}}^T \boldsymbol{N}(\boldsymbol{q}, \dot{\boldsymbol{q}}) \dot{\boldsymbol{q}} = 0; \tag{7.49}$$

notice that (7.49) does not imply (7.48), since $\boldsymbol{N}$ is a function of $\dot{\boldsymbol{q}}$, too.

It can be shown that (7.49) holds for any choice of the matrix $\boldsymbol{C}$, since it is a result of the principle of conservation of energy (*Hamilton*). By virtue of this principle, the total time derivative of kinetic energy is balanced by the power generated by all the forces acting on the manipulator joints. For the mechanical system at issue, one may write

$$\frac{1}{2}\frac{d}{dt}\left(\dot{\boldsymbol{q}}^T \boldsymbol{B}(\boldsymbol{q}) \dot{\boldsymbol{q}}\right) = \dot{\boldsymbol{q}}^T \left(\boldsymbol{\tau} - \boldsymbol{F}_v \dot{\boldsymbol{q}} - \boldsymbol{F}_s \, \mathbf{sgn}\,(\dot{\boldsymbol{q}}) - \boldsymbol{g}(\boldsymbol{q}) - \boldsymbol{J}^T(\boldsymbol{q}) \boldsymbol{h}_e\right). \tag{7.50}$$

Taking the derivative on the left-hand side of (7.50) gives

$$\frac{1}{2} \dot{\boldsymbol{q}}^T \dot{\boldsymbol{B}}(\boldsymbol{q}) \dot{\boldsymbol{q}} + \dot{\boldsymbol{q}}^T \boldsymbol{B}(\boldsymbol{q}) \ddot{\boldsymbol{q}}$$

and substituting the expression of $\boldsymbol{B}(\boldsymbol{q})\ddot{\boldsymbol{q}}$ in (7.42) yields

$$\begin{aligned} \frac{1}{2}\frac{d}{dt}\left(\dot{\boldsymbol{q}}^T \boldsymbol{B}(\boldsymbol{q}) \dot{\boldsymbol{q}}\right) = {} & \frac{1}{2} \dot{\boldsymbol{q}}^T \left(\dot{\boldsymbol{B}}(\boldsymbol{q}) - 2\boldsymbol{C}(\boldsymbol{q}, \dot{\boldsymbol{q}})\right) \dot{\boldsymbol{q}} \\ & + \dot{\boldsymbol{q}}^T \left(\boldsymbol{\tau} - \boldsymbol{F}_v \dot{\boldsymbol{q}} - \boldsymbol{F}_s \, \mathbf{sgn}\,(\dot{\boldsymbol{q}}) - \boldsymbol{g}(\boldsymbol{q}) - \boldsymbol{J}^T(\boldsymbol{q}) \boldsymbol{h}_e\right). \end{aligned} \tag{7.51}$$

A direct comparison of the right-hand sides of (7.50) and (7.51) leads to the result established by (7.49).

To summarize, the relation (7.49) holds for any choice of the matrix $\boldsymbol{C}$, since it is a direct consequence of the physical properties of the system, whereas the relation (7.48) holds only for the particular choice of the elements of $\boldsymbol{C}$ as in (7.44), (7.45).

7.2.2 Linearity in the Dynamic Parameters

An important property of the dynamic model is the *linearity* with respect to the *dynamic parameters* characterizing the manipulator links and rotors.

In order to determine such parameters, it is worth associating the kinetic and potential energy contributions of each rotor with those of the link on which it is located. Hence, by considering the union of Link i and Rotor $i+1$ (*augmented Link* i), the kinetic energy contribution is given by

$$\mathcal{T}_i = \mathcal{T}_{\ell_i} + \mathcal{T}_{m_{i+1}} \tag{7.52}$$

where

$$\mathcal{T}_{\ell_i} = \frac{1}{2} m_{\ell i} \dot{\boldsymbol{p}}_{\ell_i}^T \dot{\boldsymbol{p}}_{\ell_i} + \frac{1}{2} \boldsymbol{\omega}_i^T \boldsymbol{I}_{\ell_i} \boldsymbol{\omega}_i \tag{7.53}$$

and

$$\mathcal{T}_{m_{i+1}} = \frac{1}{2} m_{m_{i+1}} \dot{\boldsymbol{p}}_{m_{i+1}}^T \dot{\boldsymbol{p}}_{m_{i+1}} + \frac{1}{2} \boldsymbol{\omega}_{m_{i+1}}^T \boldsymbol{I}_{m_{i+1}} \boldsymbol{\omega}_{m_{i+1}}. \tag{7.54}$$

With reference to the centre of mass of the augmented link, the linear velocities of the link and rotor can be expressed according to (3.26) as

$$\dot{\boldsymbol{p}}_{\ell_i} = \dot{\boldsymbol{p}}_{C_i} + \boldsymbol{\omega}_i \times \boldsymbol{r}_{C_i,\ell_i} \tag{7.55}$$

$$\dot{\boldsymbol{p}}_{m_{i+1}} = \dot{\boldsymbol{p}}_{C_i} + \boldsymbol{\omega}_i \times \boldsymbol{r}_{C_i,m_{i+1}} \tag{7.56}$$

with

$$\boldsymbol{r}_{C_i,\ell_i} = \boldsymbol{p}_{\ell_i} - \boldsymbol{p}_{C_i} \tag{7.57}$$

$$\boldsymbol{r}_{C_i,m_{i+1}} = \boldsymbol{p}_{m_{i+1}} - \boldsymbol{p}_{C_i}, \tag{7.58}$$

where $\boldsymbol{p}_{C_i}$ denotes the position vector of the centre of mass of augmented Link i.

Substituting (7.55) into (7.53) gives

$$\begin{aligned} \mathcal{T}_{\ell_i} = {} & \frac{1}{2} m_{\ell i} \dot{\boldsymbol{p}}_{C_i}^T \dot{\boldsymbol{p}}_{C_i} + \dot{\boldsymbol{p}}_{C_i}^T \boldsymbol{S}(\boldsymbol{\omega}_i) m_{\ell_i} \boldsymbol{r}_{C_i,\ell_i} \\ & + \frac{1}{2} m_{\ell_i} \boldsymbol{\omega}_i^T \boldsymbol{S}^T(\boldsymbol{r}_{C_i,\ell_i}) \boldsymbol{S}(\boldsymbol{r}_{C_i,\ell_i}) \boldsymbol{\omega}_i + \frac{1}{2} \boldsymbol{\omega}_i^T \boldsymbol{I}_{\ell_i} \boldsymbol{\omega}_i. \end{aligned} \tag{7.59}$$

By virtue of *Steiner theorem*, the matrix

$$\bar{\boldsymbol{I}}_{\ell_i} = \boldsymbol{I}_{\ell_i} + m_{\ell_i} \boldsymbol{S}^T(\boldsymbol{r}_{C_i,\ell_i}) \boldsymbol{S}(\boldsymbol{r}_{C_i,\ell_i}) \tag{7.60}$$

represents the inertia tensor relative to the overall centre of mass $\boldsymbol{p}_{C_i}$, which contains an additional contribution due to the translation of the pole with respect to which the tensor is evaluated, as in (7.57). Therefore, (7.59) can be written as

$$\mathcal{T}_{\ell_i} = \frac{1}{2} m_{\ell i} \dot{\boldsymbol{p}}_{C_i}^T \dot{\boldsymbol{p}}_{C_i} + \dot{\boldsymbol{p}}_{C_i}^T \boldsymbol{S}(\boldsymbol{\omega}_i) m_{\ell_i} \boldsymbol{r}_{C_i,\ell_i} + \frac{1}{2} \boldsymbol{\omega}_i^T \bar{\boldsymbol{I}}_{\ell_i} \boldsymbol{\omega}_i. \tag{7.61}$$

In a similar fashion, substituting (7.56) into (7.54) and exploiting (7.23) yields

$$\begin{aligned} \mathcal{T}_{m_{i+1}} = {} & \frac{1}{2} m_{m_{i+1}} \dot{\boldsymbol{p}}_{C_i}^T \dot{\boldsymbol{p}}_{C_i} + \dot{\boldsymbol{p}}_{C_i}^T \boldsymbol{S}(\boldsymbol{\omega}_i) m_{m_{i+1}} \boldsymbol{r}_{C_i,m_{i+1}} + \frac{1}{2} \boldsymbol{\omega}_i^T \bar{\boldsymbol{I}}_{m_{i+1}} \boldsymbol{\omega}_i \\ & + k_{r,i+1} \dot{q}_{i+1} \boldsymbol{z}_{m_{i+1}}^T \boldsymbol{I}_{m_{i+1}} \boldsymbol{\omega}_i + \frac{1}{2} k_{r,i+1}^2 \dot{q}_{i+1}^2 \boldsymbol{z}_{m_{i+1}}^T \boldsymbol{I}_{m_{i+1}} \boldsymbol{z}_{m_{i+1}}, \end{aligned} \tag{7.62}$$

where

$$\bar{\boldsymbol{I}}_{m_{i+1}} = \boldsymbol{I}_{m_{i+1}} + m_{m_{i+1}} \boldsymbol{S}^T(\boldsymbol{r}_{C_i,m_{i+1}}) \boldsymbol{S}(\boldsymbol{r}_{C_i,m_{i+1}}). \tag{7.63}$$

Summing the contributions in (7.61), (7.62) as in (7.52) gives the expression of the kinetic energy of augmented Link i in the form

$$\mathcal{T}_i = \frac{1}{2} m_i \dot{\boldsymbol{p}}_{C_i}^T \dot{\boldsymbol{p}}_{C_i} + \frac{1}{2} \boldsymbol{\omega}_i^T \bar{\boldsymbol{I}}_i \boldsymbol{\omega}_i + k_{r,i+1} \dot{q}_{i+1} \boldsymbol{z}_{m_{i+1}}^T \boldsymbol{I}_{m_{i+1}} \boldsymbol{\omega}_i + \frac{1}{2} k_{r,i+1}^2 \dot{q}_{i+1}^2 \boldsymbol{z}_{m_{i+1}}^T \boldsymbol{I}_{m_{i+1}} \boldsymbol{z}_{m_{i+1}}, \tag{7.64}$$

where $m_i = m_{\ell_i} + m_{m_{i+1}}$ and $\bar{\boldsymbol{I}}_i = \bar{\boldsymbol{I}}_{\ell_i} + \bar{\boldsymbol{I}}_{m_{i+1}}$ are respectively the overall mass and inertia tensor. In deriving (7.64), the relations in (7.57), (7.58) have been utilized as well as the following relation between the positions of the centres of mass:

$$m_{\ell_i} \boldsymbol{p}_{\ell_i} + m_{m_{i+1}} \boldsymbol{p}_{m_{i+1}} = m_i \boldsymbol{p}_{C_i}. \tag{7.65}$$

Notice that the first two terms on the right-hand side of (7.64) represent the kinetic energy contribution of the rotor when this is still, whereas the remaining two terms account for the rotor's own motion.

On the assumption that the rotor has a symmetric mass distribution about its axis of rotation, its inertia tensor expressed in a frame $\boldsymbol{R}_{m_i}$ with origin at the centre of mass and axis z_{m_i} aligned with the rotation axis can be written as

$$\boldsymbol{I}_{m_i}^{m_i} = \begin{bmatrix} I_{m_i xx} & 0 & 0 \\ 0 & I_{m_i yy} & 0 \\ 0 & 0 & I_{m_i zz} \end{bmatrix} \tag{7.66}$$

where $I_{m_i yy} = I_{m_i xx}$. As a consequence, the inertia tensor is invariant with respect to any rotation about axis z_{m_i} and is, anyhow, constant when referred to any frame attached to Link $i-1$.

Since the aim is to determine a set of dynamic parameters independent of the manipulator joint configuration, it is worth referring the inertia tensor of the link $\bar{\boldsymbol{I}}_i$ to frame $\boldsymbol{R}_i$ attached to the link and the inertia tensor $\boldsymbol{I}_{m_{i+1}}$ to frame $\boldsymbol{R}_{m_{i+1}}$ so that it is diagonal. In view of (7.66) one has

$$\boldsymbol{I}_{m_{i+1}} \boldsymbol{z}_{m_{i+1}} = \boldsymbol{R}_{m_{i+1}} \boldsymbol{I}_{m_{i+1}}^{m_{i+1}} \boldsymbol{R}_{m_{i+1}}^T \boldsymbol{z}_{m_{i+1}} = I_{m_{i+1}} \boldsymbol{z}_{m_{i+1}} \tag{7.67}$$

where $I_{m_{i+1}} = I_{m_{i+1} zz}$ denotes the constant scalar moment of inertia of the rotor about its rotation axis.

Therefore, the kinetic energy (7.64) becomes

$$\mathcal{T}_i = \frac{1}{2} m_i \dot{\boldsymbol{p}}_{C_i}^{iT} \dot{\boldsymbol{p}}_{C_i}^i + \frac{1}{2} \boldsymbol{\omega}_i^{iT} \bar{\boldsymbol{I}}_i^i \boldsymbol{\omega}_i^i + k_{r,i+1} \dot{q}_{i+1} I_{m_{i+1}} \boldsymbol{z}_{m_{i+1}}^{iT} \boldsymbol{\omega}_i^i + \frac{1}{2} k_{r,i+1}^2 \dot{q}_{i+1}^2 I_{m_{i+1}}. \tag{7.68}$$

According to the linear velocity composition rule for Link i in (3.15), one may write

$$\dot{\boldsymbol{p}}_{C_i}^i = \dot{\boldsymbol{p}}_i^i + \boldsymbol{\omega}_i^i \times \boldsymbol{r}_{i,C_i}^i, \tag{7.69}$$

where all the vectors have been referred to Frame i; note that $\boldsymbol{r}^i_{i,C_i}$ is fixed in such a frame. Substituting (7.69) into (7.68) gives

$$\begin{aligned}\mathcal{T}_i = \frac{1}{2} m_i \dot{\boldsymbol{p}}_i^{iT} \dot{\boldsymbol{p}}_i^i + \dot{\boldsymbol{p}}_i^{iT} \boldsymbol{S}(\boldsymbol{\omega}_i^i) m_i \boldsymbol{r}^i_{i,C_i} + \frac{1}{2} \boldsymbol{\omega}_i^{iT} \widehat{\boldsymbol{I}}_i^i \boldsymbol{\omega}_i^i \\ + k_{r,i+1} \dot{q}_{i+1} I_{m_{i+1}} \boldsymbol{z}_{m_{i+1}}^{iT} \boldsymbol{\omega}_i^i + \frac{1}{2} k_{r,i+1}^2 \dot{q}_{i+1}^2 I_{m_{i+1}},\end{aligned} \tag{7.70}$$

where

$$\widehat{\boldsymbol{I}}_i^i = \bar{\boldsymbol{I}}_i^i + m_i \boldsymbol{S}^T(\boldsymbol{r}^i_{i,C_i}) \boldsymbol{S}(\boldsymbol{r}^i_{i,C_i}) \tag{7.71}$$

represents the inertia tensor with respect to the origin of Frame i according to Steiner theorem.

Let $\boldsymbol{r}^i_{i,C_i} = [\, \ell_{C_i x} \quad \ell_{C_i y} \quad \ell_{C_i z} \,]^T$. The *first moment of inertia* is

$$m_i \boldsymbol{r}^i_{i,C_i} = \begin{bmatrix} m_i \ell_{C_i x} \\ m_i \ell_{C_i y} \\ m_i \ell_{C_i z} \end{bmatrix}. \tag{7.72}$$

From (7.71) the inertia tensor of augmented Link i is

$$\begin{aligned}\widehat{\boldsymbol{I}}_i^i &= \begin{bmatrix} \bar{I}_{ixx} + m_i(\ell_{C_i y}^2 + \ell_{C_i z}^2) & -\bar{I}_{ixy} - m_i \ell_{C_i x} \ell_{C_i y} & -\bar{I}_{ixz} - m_i \ell_{C_i x} \ell_{C_i z} \\ * & \bar{I}_{iyy} + m_i(\ell_{C_i x}^2 + \ell_{C_i z}^2) & -\bar{I}_{iyz} - m_i \ell_{C_i y} \ell_{C_i z} \\ * & * & \bar{I}_{izz} + m_i(\ell_{C_i x}^2 + \ell_{C_i y}^2) \end{bmatrix} \\ &= \begin{bmatrix} \widehat{I}_{ixx} & -\widehat{I}_{ixy} & -\widehat{I}_{ixz} \\ * & \widehat{I}_{iyy} & -\widehat{I}_{iyz} \\ * & * & \widehat{I}_{izz} \end{bmatrix}.\end{aligned} \tag{7.73}$$

Therefore, the kinetic energy of the augmented link is linear with respect to the dynamic parameters, namely, the *mass*, the *three components of the first moment of inertia* in (7.72), the *six components of the inertia tensor* in (7.73), and the *moment of inertia of the rotor*.

As regards potential energy, it is worth referring to the centre of mass of augmented Link i defined as in (7.65), and thus the single contribution of potential energy can be written as

$$\mathcal{U}_i = -m_i \boldsymbol{g}_0^{iT} \boldsymbol{p}^i_{C_i} \tag{7.74}$$

where the vectors have been referred to Frame i. According to the relation

$$\boldsymbol{p}^i_{C_i} = \boldsymbol{p}^i_i + \boldsymbol{r}^i_{i,C_i}.$$

The expression in (7.74) can be rewritten as

$$\mathcal{U}_i = -\boldsymbol{g}_0^{iT} (m_i \boldsymbol{p}^i_i + m_i \boldsymbol{r}^i_{i,C_i}) \tag{7.75}$$

that is, the potential energy of the augmented link is linear with respect to the mass and the three components of the first moment of inertia in (7.72).

By summing the contributions of kinetic energy and potential energy for all augmented links, the Lagrangian of the system (7.1) can be expressed in the form

$$\mathcal{L} = \sum_{i=1}^{n} (\boldsymbol{\beta}_{\mathcal{T}i}^T - \boldsymbol{\beta}_{\mathcal{U}i}^T)\boldsymbol{\pi}_i \tag{7.76}$$

where $\boldsymbol{\pi}_i$ is the (11×1) vector of dynamic parameters

$$\boldsymbol{\pi}_i = [\, m_i \;\; m_i\ell_{C_ix} \;\; m_i\ell_{C_iy} \;\; m_i\ell_{C_iz} \;\; \widehat{I}_{ixx} \;\; \widehat{I}_{ixy} \;\; \widehat{I}_{ixz} \;\; \widehat{I}_{iyy} \;\; \widehat{I}_{iyz} \;\; \widehat{I}_{izz} \;\; I_{m_i}\,]^T, \tag{7.77}$$

in which the moment of inertia of Rotor i has been associated with the parameters of Link i so as to simplify the notation.

In (7.76), $\boldsymbol{\beta}_{\mathcal{T}i}$ and $\boldsymbol{\beta}_{\mathcal{U}i}$ are two (11×1) vectors that allow the Lagrangian to be written as a function of $\boldsymbol{\pi}_i$. Such vectors are a function of the generalized coordinates of the mechanical system (and also of their derivatives as regards $\boldsymbol{\beta}_{\mathcal{T}i}$). In particular, it can be shown that $\boldsymbol{\beta}_{\mathcal{T}i} = \boldsymbol{\beta}_{\mathcal{T}i}(q_1, q_2, \ldots, q_i, \dot{q}_1, \dot{q}_2, \ldots, \dot{q}_i)$ and $\boldsymbol{\beta}_{\mathcal{U}i} = \boldsymbol{\beta}_{\mathcal{U}i}(q_1, q_2, \ldots, q_i)$, i.e., they do not depend on the variables of the joints subsequent to Link i.

At this point, it should be observed how the derivations required by the Lagrange equations in (7.2) do not alter the property of linearity in the parameters, and then the generalized force at Joint i can be written as

$$\xi_i = \sum_{j=1}^{n} \boldsymbol{y}_{ij}^T \boldsymbol{\pi}_j \tag{7.78}$$

where

$$\boldsymbol{y}_{ij} = \frac{d}{dt}\frac{\partial \boldsymbol{\beta}_{\mathcal{T}j}}{\partial \dot{q}_i} - \frac{\partial \boldsymbol{\beta}_{\mathcal{T}j}}{\partial q_i} + \frac{\partial \boldsymbol{\beta}_{\mathcal{U}j}}{\partial q_i}. \tag{7.79}$$

Since the partial derivatives of $\boldsymbol{\beta}_{\mathcal{T}j}$ and $\boldsymbol{\beta}_{\mathcal{U}j}$ appearing in (7.79) vanish for $j < i$, the following notable result is obtained:

$$\begin{bmatrix} \xi_1 \\ \xi_2 \\ \vdots \\ \xi_n \end{bmatrix} = \begin{bmatrix} \boldsymbol{y}_{11}^T & \boldsymbol{y}_{12}^T & \cdots & \boldsymbol{y}_{1n}^T \\ \mathbf{0}^T & \boldsymbol{y}_{22}^T & \cdots & \boldsymbol{y}_{2n}^T \\ \vdots & \vdots & \ddots & \vdots \\ \mathbf{0}^T & \mathbf{0}^T & \ldots & \boldsymbol{y}_{nn}^T \end{bmatrix} \begin{bmatrix} \boldsymbol{\pi}_1 \\ \boldsymbol{\pi}_2 \\ \vdots \\ \boldsymbol{\pi}_n \end{bmatrix} \tag{7.80}$$

which yields the property of *linearity of the model* of a manipulator with respect to a suitable set of *dynamic parameters*.

In the simple case of no contact forces ($\boldsymbol{h}_e = \mathbf{0}$), it may be worth including the viscous friction coefficient F_{vi} and Coulomb friction coefficient F_{si} in the parameters of the vector $\boldsymbol{\pi}_i$, thus leading to a total number of 13 parameters per joint. In summary, (7.80) can be compactly written as

$$\boldsymbol{\tau} = \boldsymbol{Y}(\boldsymbol{q}, \dot{\boldsymbol{q}}, \ddot{\boldsymbol{q}})\boldsymbol{\pi} \tag{7.81}$$

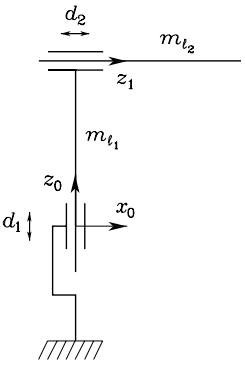

Fig. 7.3. Two-link Cartesian arm

where $\boldsymbol{\pi}$ is a $(p \times 1)$ vector of *constant* parameters and $\boldsymbol{Y}$ is an $(n \times p)$ matrix which is a *function of joint positions, velocities and accelerations*; this matrix is usually called *regressor*. Regarding the dimension of the parameter vector, notice that $p \leq 13n$ since not all the thirteen parameters for each joint may explicitly appear in (7.81).

7.3 Dynamic Model of Simple Manipulator Structures

In the following, three examples of dynamic model computation are illustrated for simple two-DOF manipulator structures. Two DOFs, in fact, are enough to understand the physical meaning of all dynamic terms, especially the joint coupling terms. On the other hand, dynamic model computation for manipulators with more DOFs would be quite tedious and prone to errors, when carried out by paper and pencil. In those cases, it is advisable to perform it with the aid of a symbolic programming software package.

7.3.1 Two-link Cartesian Arm

Consider the two-link Cartesian arm in Fig. 7.3, for which the vector of generalized coordinates is $\boldsymbol{q} = [\, d_1 \quad d_2 \,]^T$. Let m_{ℓ_1}, m_{ℓ_2} be the masses of the two links, and m_{m_1}, m_{m_2} the masses of the rotors of the two joint motors. Also let I_{m_1}, I_{m_2} be the moments of inertia with respect to the axes of the two rotors. It is assumed that $\boldsymbol{p}_{m_i} = \boldsymbol{p}_{i-1}$ and $\boldsymbol{z}_{m_i} = \boldsymbol{z}_{i-1}$, for $i = 1, 2$, i.e., the motors are located on the joint axes with centres of mass located at the origins of the respective frames.

With the chosen coordinate frames, computation of the Jacobians in (7.16), (7.18) yields

$$\boldsymbol{J}_P^{(\ell_1)} = \begin{bmatrix} 0 & 0 \\ 0 & 0 \\ 1 & 0 \end{bmatrix} \qquad \boldsymbol{J}_P^{(\ell_2)} = \begin{bmatrix} 0 & 1 \\ 0 & 0 \\ 1 & 0 \end{bmatrix}.$$

Obviously, in this case there are no angular velocity contributions for both links.

Computation of the Jacobians in (7.25), (7.26) e (7.28), (7.29) yields

$$\boldsymbol{J}_P^{(m_1)} = \begin{bmatrix} 0 & 0 \\ 0 & 0 \\ 0 & 0 \end{bmatrix} \qquad \boldsymbol{J}_P^{(m_2)} = \begin{bmatrix} 0 & 0 & \\ 0 & 0 & 1 & 0 \end{bmatrix}$$

$$\boldsymbol{J}_O^{(m_1)} = \begin{bmatrix} 0 & 0 \\ 0 & 0 \\ k_{r1} & 0 \end{bmatrix} \qquad \boldsymbol{J}_O^{(m_2)} = \begin{bmatrix} 0 & k_{r2} \\ 0 & 0 \\ 0 & 0 \end{bmatrix}$$

where k_{ri} is the gear reduction ratio of Motor i. It is obvious to see that $\boldsymbol{z}_1 = [\,1 \quad 0 \quad 0\,]^T$, which greatly simplifies computation of the second term in (7.30).

From (7.32), the inertia matrix is

$$\boldsymbol{B} = \begin{bmatrix} m_{\ell_1} + m_{m_2} + k_{r1}^2 I_{m_1} + m_{\ell_2} & 0 \\ 0 & m_{\ell_2} + k_{r2}^2 I_{m_2} \end{bmatrix}.$$

It is worth observing that $\boldsymbol{B}$ is *constant*, i.e., it does not depend on the arm configuration. This implies also that $\boldsymbol{C} = \boldsymbol{O}$, i.e., there are no contributions of centrifugal and Coriolis forces. As for the gravitational terms, since $\boldsymbol{g}_0 = [\,0 \quad 0 \quad -g\,]^T$ (g is gravity acceleration), (7.39) with the above Jacobians gives

$$g_1 = (m_{\ell_1} + m_{m_2} + m_{\ell_2})g \qquad g_2 = 0.$$

In the absence of friction and tip contact forces, the resulting equations of motion are

$$\begin{aligned} (m_{\ell_1} + m_{m_2} + k_{r1}^2 I_{m_1} + m_{\ell_2})\ddot{d}_1 + (m_{\ell_1} + m_{m_2} + m_{\ell_2})g &= \tau_1 \\ (m_{\ell_2} + k_{r2}^2 I_{m_2})\ddot{d}_2 &= \tau_2 \end{aligned}$$

where τ_1 and τ_2 denote the forces applied to the two joints. Notice that a completely decoupled dynamics has been obtained. This is a consequence not only of the Cartesian structures but also of the particular geometry; in other words, if the second joint axis were not at a right angle with the first joint axis, the resulting inertia matrix would not be diagonal (see Problem 7.1).

7.3.2 Two-link Planar Arm

Consider the two-link planar arm in Fig. 7.4, for which the vector of generalized coordinates is $\boldsymbol{q} = [\,\vartheta_1 \quad \vartheta_2\,]^T$. Let ℓ_1, ℓ_2 be the distances of the centres of mass of the two links from the respective joint axes. Also let m_{ℓ_1}, m_{ℓ_2} be the masses of the two links, and m_{m_1}, m_{m_2} the masses of the rotors of the two joint motors. Finally, let I_{m_1}, I_{m_2} be the moments of inertia with respect to the axes of the two rotors, and I_{ℓ_1}, I_{ℓ_2} the moments of inertia relative to the

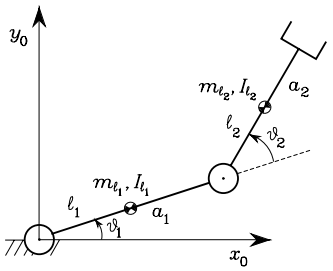

Fig. 7.4. Two-link planar arm

centres of mass of the two links, respectively. It is assumed that $\boldsymbol{p}_{m_i} = \boldsymbol{p}_{i-1}$ and $\boldsymbol{z}_{m_i} = \boldsymbol{z}_{i-1}$, for $i = 1, 2$, i.e., the motors are located on the joint axes with centres of mass located at the origins of the respective frames.

With the chosen coordinate frames, computation of the Jacobians in (7.16), (7.18) yields

$$\boldsymbol{J}_P^{(\ell_1)} = \begin{bmatrix} -\ell_1 s_1 & 0 \\ \ell_1 c_1 & 0 \\ 0 & 0 \end{bmatrix} \qquad \boldsymbol{J}_P^{(\ell_2)} = \begin{bmatrix} -a_1 s_1 - \ell_2 s_{12} & -\ell_2 s_{12} \\ a_1 c_1 + \ell_2 c_{12} & \ell_2 c_{12} \\ 0 & 0 \end{bmatrix},$$

whereas computation of the Jacobians in (7.17), (7.19) yields

$$\boldsymbol{J}_O^{(\ell_1)} = \begin{bmatrix} 0 & 0 \\ 0 & 0 \\ 1 & 0 \end{bmatrix} \qquad \boldsymbol{J}_O^{(\ell_2)} = \begin{bmatrix} 0 & 0 \\ 0 & 0 \\ 1 & 1 \end{bmatrix}.$$

Notice that $\boldsymbol{\omega}_i$, for $i = 1, 2$, is aligned with z_0, and thus $\boldsymbol{R}_i$ has *no* effect. It is then possible to refer to the scalar moments of inertia I_{ℓ_i}.

Computation of the Jacobians in (7.25), (7.26) yields

$$\boldsymbol{J}_P^{(m_1)} = \begin{bmatrix} 0 & 0 \\ 0 & 0 \\ 0 & 0 \end{bmatrix} \qquad \boldsymbol{J}_P^{(m_2)} = \begin{bmatrix} -a_1 s_1 & 0 \\ a_1 c_1 & 0 \\ 0 & 0 \end{bmatrix},$$

whereas computation of the Jacobians in (7.28), (7.29) yields

$$\boldsymbol{J}_O^{(m_1)} = \begin{bmatrix} 0 & 0 \\ 0 & 0 \\ k_{r1} & 0 \end{bmatrix} \qquad \boldsymbol{J}_O^{(m_2)} = \begin{bmatrix} 0 & 0 \\ 0 & 0 \\ 1 & k_{r2} \end{bmatrix}$$

where k_{ri} is the gear reduction ratio of Motor i.

From (7.32), the inertia matrix is

$$\boldsymbol{B}(\boldsymbol{q}) = \begin{bmatrix} b_{11}(\vartheta_2) & b_{12}(\vartheta_2) \\ b_{21}(\vartheta_2) & b_{22} \end{bmatrix}$$

$$
\begin{aligned}
b_{11} &= I_{\ell_1} + m_{\ell_1}\ell_1^2 + k_{r1}^2 I_{m_1} + I_{\ell_2} + m_{\ell_2}(a_1^2 + \ell_2^2 + 2a_1\ell_2 c_2) \\
&\quad + I_{m_2} + m_{m_2} a_1^2 \\
b_{12} &= b_{21} = I_{\ell_2} + m_{\ell_2}(\ell_2^2 + a_1\ell_2 c_2) + k_{r2} I_{m_2} \\
b_{22} &= I_{\ell_2} + m_{\ell_2}\ell_2^2 + k_{r2}^2 I_{m_2}.
\end{aligned}
$$

Compared to the previous example, the inertia matrix is now configuration-dependent. Notice that the term $k_{r2}I_{m_2}$ in the off-diagonal term of the inertia matrix derives from having considered the rotational part of the motor kinetic energy as due to the total angular velocity, i.e., its own angular velocity and that of the preceding link in the kinematic chain. At first approximation, especially in the case of high values of the gear reduction ratio, this contribution could be neglected; in the resulting reduced model, motor inertias would appear uniquely in the elements on the diagonal of the inertia matrix with terms of the type $k_{ri}^2 I_{m_i}$.

The computation of Christoffel symbols as in (7.45) gives

$$
\begin{aligned}
c_{111} &= \frac{1}{2}\frac{\partial b_{11}}{\partial q_1} = 0 \\
c_{112} &= c_{121} = \frac{1}{2}\frac{\partial b_{11}}{\partial q_2} = -m_{\ell_2} a_1 \ell_2 s_2 = h \\
c_{122} &= \frac{\partial b_{12}}{\partial q_2} - \frac{1}{2}\frac{\partial b_{22}}{\partial q_1} = h \\
c_{211} &= \frac{\partial b_{21}}{\partial q_1} - \frac{1}{2}\frac{\partial b_{11}}{\partial q_2} = -h \\
c_{212} &= c_{221} = \frac{1}{2}\frac{\partial b_{22}}{\partial q_1} = 0 \\
c_{222} &= \frac{1}{2}\frac{\partial b_{22}}{\partial q_2} = 0,
\end{aligned}
$$

leading to the matrix

$$
\boldsymbol{C}(\boldsymbol{q}, \dot{\boldsymbol{q}}) = \begin{bmatrix} h\dot{\vartheta}_2 & h(\dot{\vartheta}_1 + \dot{\vartheta}_2) \\ -h\dot{\vartheta}_1 & 0 \end{bmatrix}.
$$

Computing the matrix $\boldsymbol{N}$ in (7.47) gives

$$
\begin{aligned}
\boldsymbol{N}(\boldsymbol{q}, \dot{\boldsymbol{q}}) &= \dot{\boldsymbol{B}}(\boldsymbol{q}) - 2\boldsymbol{C}(\boldsymbol{q}, \dot{\boldsymbol{q}}) \\
&= \begin{bmatrix} 2h\dot{\vartheta}_2 & h\dot{\vartheta}_2 \\ h\dot{\vartheta}_2 & 0 \end{bmatrix} - 2\begin{bmatrix} h\dot{\vartheta}_2 & h(\dot{\vartheta}_1 + \dot{\vartheta}_2) \\ -h\dot{\vartheta}_1 & 0 \end{bmatrix} \\
&= \begin{bmatrix} 0 & -2h\dot{\vartheta}_1 - h\dot{\vartheta}_2 \\ 2h\dot{\vartheta}_1 + h\dot{\vartheta}_2 & 0 \end{bmatrix}
\end{aligned}
$$

that allows the verification of the skew-symmetry property expressed by (7.48). See also Problem 7.2.

As for the gravitational terms, since $\boldsymbol{g}_0 = [\,0 \quad -g \quad 0\,]^T$, (7.39) with the above Jacobians gives

$$\begin{aligned} g_1 &= (m_{\ell_1}\ell_1 + m_{m_2}a_1 + m_{\ell_2}a_1)gc_1 + m_{\ell_2}\ell_2 g c_{12} \\ g_2 &= m_{\ell_2}\ell_2 g c_{12}. \end{aligned}$$

In the absence of friction and tip contact forces, the resulting equations of motion are

$$\begin{aligned} &\left(I_{\ell_1} + m_{\ell_1}\ell_1^2 + k_{r1}^2 I_{m_1} + I_{\ell_2} + m_{\ell_2}(a_1^2 + \ell_2^2 + 2a_1\ell_2 c_2) + I_{m_2} + m_{m_2}a_1^2\right)\ddot{\vartheta}_1 \\ &\quad + \left(I_{\ell_2} + m_{\ell_2}(\ell_2^2 + a_1\ell_2 c_2) + k_{r2}I_{m_2}\right)\ddot{\vartheta}_2 \\ &\quad -2m_{\ell_2}a_1\ell_2 s_2\dot{\vartheta}_1\dot{\vartheta}_2 - m_{\ell_2}a_1\ell_2 s_2\dot{\vartheta}_2^2 \\ &\quad +(m_{\ell_1}\ell_1 + m_{m_2}a_1 + m_{\ell_2}a_1)gc_1 + m_{\ell_2}\ell_2 g c_{12} = \tau_1 \\ &\left(I_{\ell_2} + m_{\ell_2}(\ell_2^2 + a_1\ell_2 c_2) + k_{r2}I_{m_2}\right)\ddot{\vartheta}_1 + \left(I_{\ell_2} + m_{\ell_2}\ell_2^2 + k_{r2}^2 I_{m_2}\right)\ddot{\vartheta}_2 \\ &\quad +m_{\ell_2}a_1\ell_2 s_2\dot{\vartheta}_1^2 + m_{\ell_2}\ell_2 g c_{12} = \tau_2 \end{aligned} \tag{7.82}$$

where τ_1 and τ_2 denote the torques applied to the joints.

Finally, it is wished to derive a parameterization of the dynamic model (7.82) according to the relation (7.81). By direct inspection of the expressions of the joint torques, it is possible to find the following parameter vector:

$$\boldsymbol{\pi} = [\,\pi_1 \quad \pi_2 \quad \pi_3 \quad \pi_4 \quad \pi_5 \quad \pi_6 \quad \pi_7 \quad \pi_8\,]^T \tag{7.83}$$

$$\begin{aligned} \pi_1 &= m_1 = m_{\ell_1} + m_{m_2} \\ \pi_2 &= m_1\ell_{C_1} = m_{\ell_1}(\ell_1 - a_1) \\ \pi_3 &= \widehat{I}_1 = I_{\ell_1} + m_{\ell_1}(\ell_1 - a_1)^2 + I_{m_2} \\ \pi_4 &= I_{m_1} \\ \pi_5 &= m_2 = m_{\ell_2} \\ \pi_6 &= m_2\ell_{C_2} = m_{\ell_2}(\ell_2 - a_2) \\ \pi_7 &= \widehat{I}_2 = I_{\ell_2} + m_{\ell_2}(\ell_2 - a_2)^2 \\ \pi_8 &= I_{m_2}, \end{aligned}$$

where the parameters for the augmented links have been found according to (7.77). It can be recognized that the number of non-null parameters is less than the maximum number of twenty-two parameters allowed in this case.[6] The regressor in (7.81) is

$$\boldsymbol{Y} = \begin{bmatrix} y_{11} & y_{12} & y_{13} & y_{14} & y_{15} & y_{16} & y_{17} & y_{18} \\ y_{21} & y_{22} & y_{23} & y_{24} & y_{25} & y_{26} & y_{27} & y_{28} \end{bmatrix} \tag{7.84}$$

[6] The number of parameters can be further reduced by resorting to a more accurate inspection, which leads to finding a minimum number of five parameters; those turn out to be a linear combination of the parameters in (7.83) (see Problem 7.4).

$$
\begin{aligned}
y_{11} &= a_1^2\ddot{\vartheta}_1 + a_1 g c_1 \\
y_{12} &= 2a_1\ddot{\vartheta}_1 + g c_1 \\
y_{13} &= \ddot{\vartheta}_1 \\
y_{14} &= k_{r1}^2\ddot{\vartheta}_1 \\
y_{15} &= (a_1^2 + 2a_1a_2c_2 + a_2^2)\ddot{\vartheta}_1 + (a_1a_2c_2 + a_2^2)\ddot{\vartheta}_2 - 2a_1a_2s_2\dot{\vartheta}_1\dot{\vartheta}_2 \\
&\quad -a_1a_2s_2\dot{\vartheta}_2^2 + a_1gc_1 + a_2gc_{12} \\
y_{16} &= (2a_1c_2 + 2a_2)\ddot{\vartheta}_1 + (a_1c_2 + 2a_2)\ddot{\vartheta}_2 - 2a_1s_2\dot{\vartheta}_1\dot{\vartheta}_2 - a_1s_2\dot{\vartheta}_2^2 \\
&\quad +gc_{12} \\
y_{17} &= \ddot{\vartheta}_1 + \ddot{\vartheta}_2 \\
y_{18} &= k_{r2}\ddot{\vartheta}_2
\end{aligned}
$$

$$
\begin{aligned}
y_{21} &= 0 \\
y_{22} &= 0 \\
y_{23} &= 0 \\
y_{24} &= 0 \\
y_{25} &= (a_1a_2c_2 + a_2^2)\ddot{\vartheta}_1 + a_2^2\ddot{\vartheta}_2 + a_1a_2s_2\dot{\vartheta}_1^2 + a_2gc_{12} \\
y_{26} &= (a_1c_2 + 2a_2)\ddot{\vartheta}_1 + 2a_2\ddot{\vartheta}_2 + a_1s_2\dot{\vartheta}_1^2 + gc_{12} \\
y_{27} &= \ddot{\vartheta}_1 + \ddot{\vartheta}_2 \\
y_{28} &= k_{r2}\ddot{\vartheta}_1 + k_{r2}^2\ddot{\vartheta}_2.
\end{aligned}
$$

Example 7.2

In order to understand the relative weight of the various torque contributions in the dynamic model (7.82), consider a two-link planar arm with the following data:

$$a_1 = a_2 = 1\,\mathrm{m} \quad \ell_1 = \ell_2 = 0.5\,\mathrm{m} \quad m_{\ell_1} = m_{\ell_2} = 50\,\mathrm{kg} \quad I_{\ell_1} = I_{\ell_2} = 10\,\mathrm{kg{\cdot}m^2}$$

$$k_{r1} = k_{r2} = 100 \quad m_{m_1} = m_{m_2} = 5\,\mathrm{kg} \quad I_{m_1} = I_{m_2} = 0.01\,\mathrm{kg{\cdot}m^2}.$$

The two links have been chosen equal to illustrate better the dynamic interaction between the two joints.

Figure 7.5 shows the time history of positions, velocities, accelerations and torques resulting from joint trajectories with typical triangular velocity profile and equal time duration. The initial arm configuration is so that the tip is located at the point $(0.2, 0)\,\mathrm{m}$ with a lower elbow posture. Both joints make a rotation of $\pi/2\,\mathrm{rad}$ in a time of $0.5\,\mathrm{s}$.

From the time history of the single torque contributions in Fig. 7.6 it can be recognized that:

- The inertia torque at Joint 1 due to Joint 1 acceleration follows the time history of the acceleration.
- The inertia torque at Joint 2 due to Joint 2 acceleration is piecewise constant, since the inertia moment at Joint 2 axis is constant.

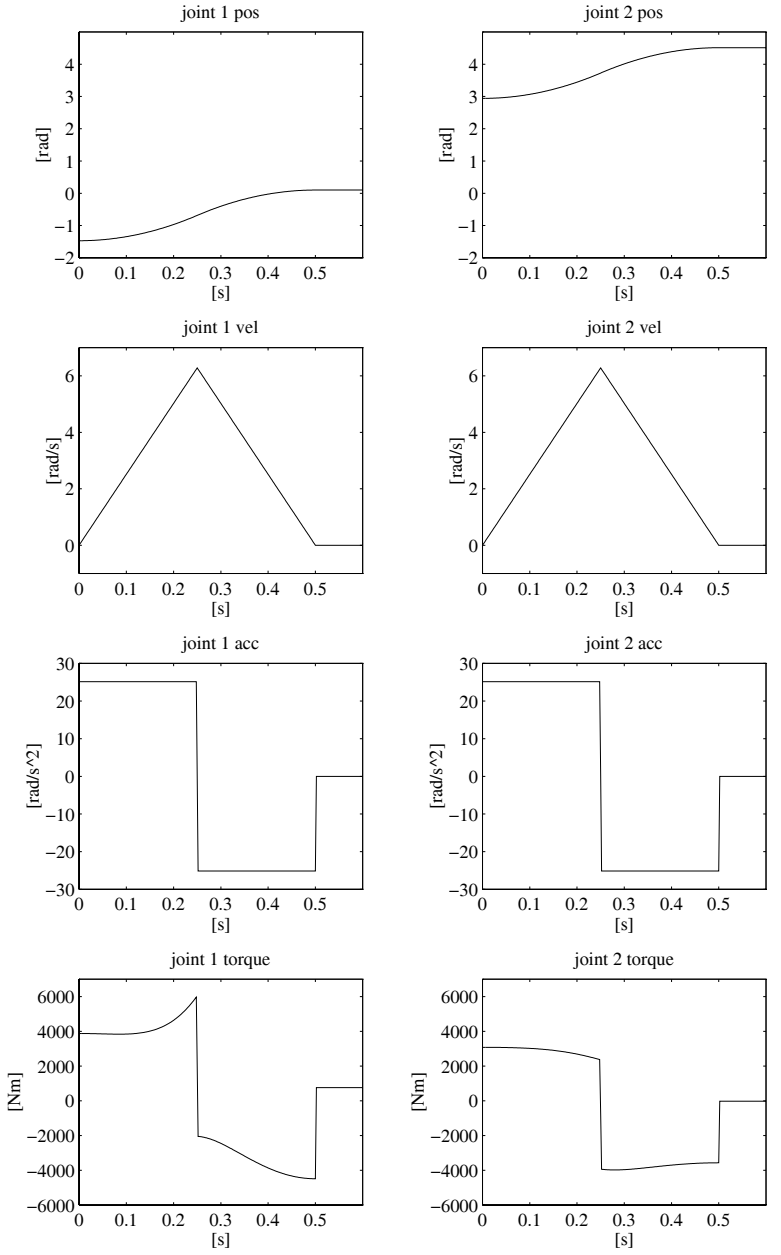

Fig. 7.5. Time history of positions, velocities, accelerations and torques with joint trajectories of equal duration

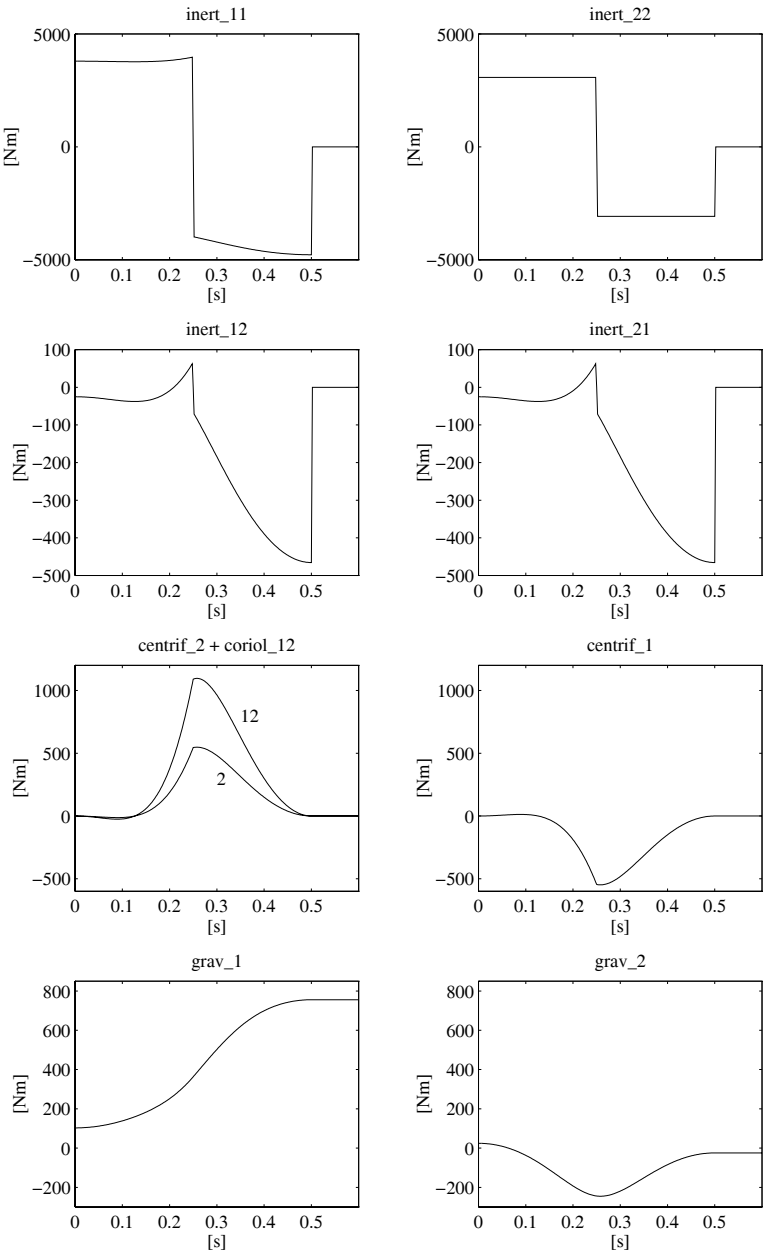

Fig. 7.6. Time history of torque contributions with joint trajectories of equal duration

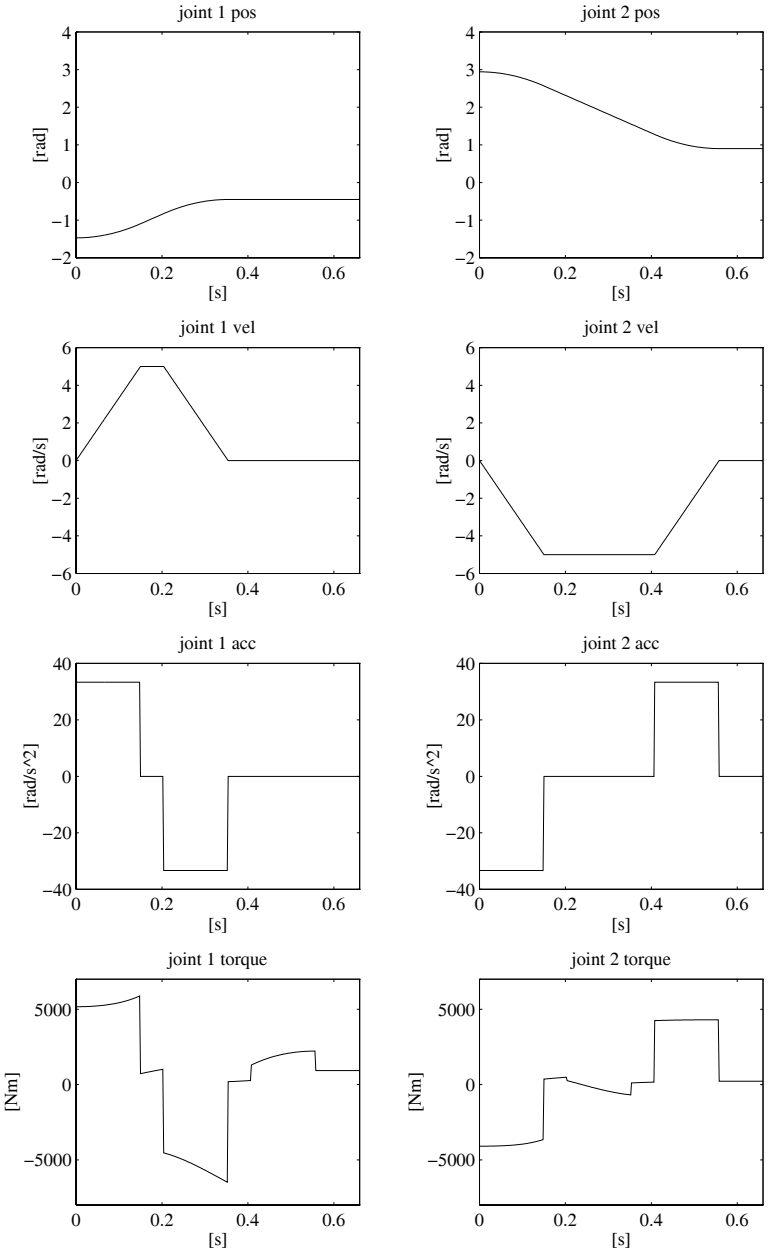

Fig. 7.7. Time history of positions, velocities, accelerations and torques with joint trajectories of different duration

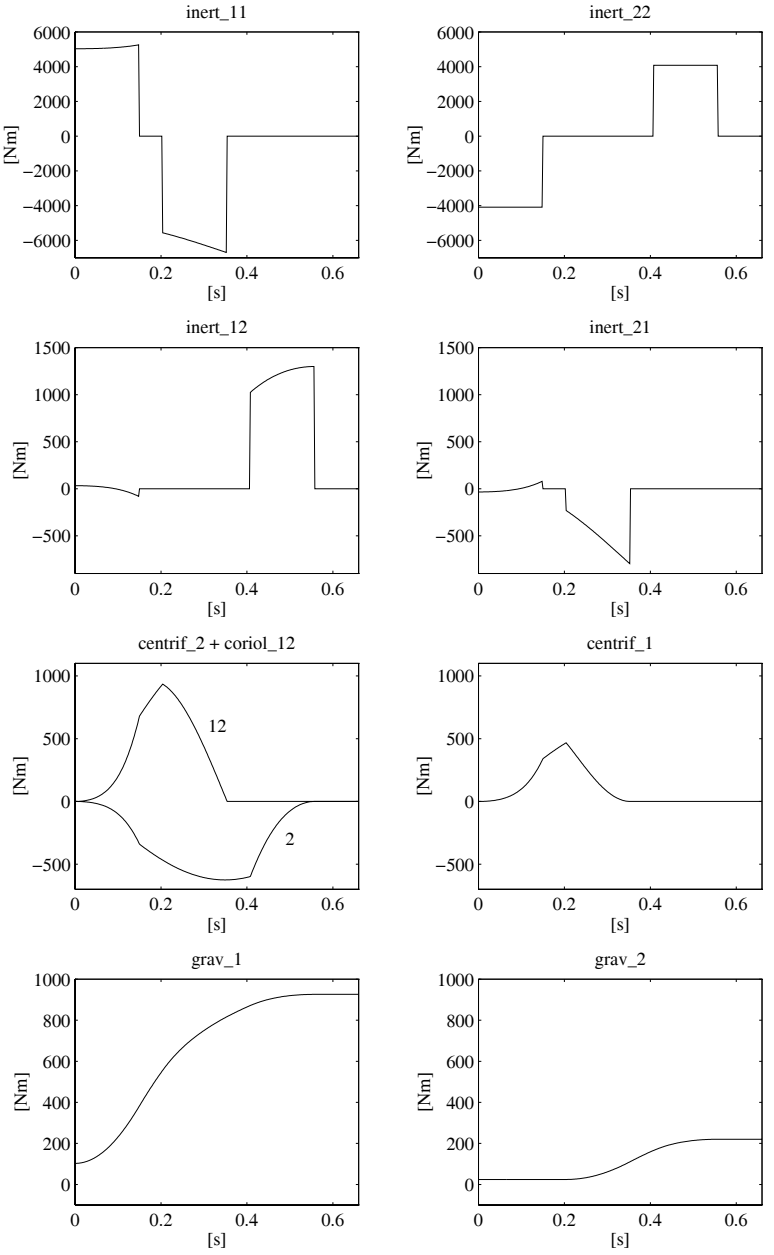

Fig. 7.8. Time history of torque contributions with joint trajectories of different duration

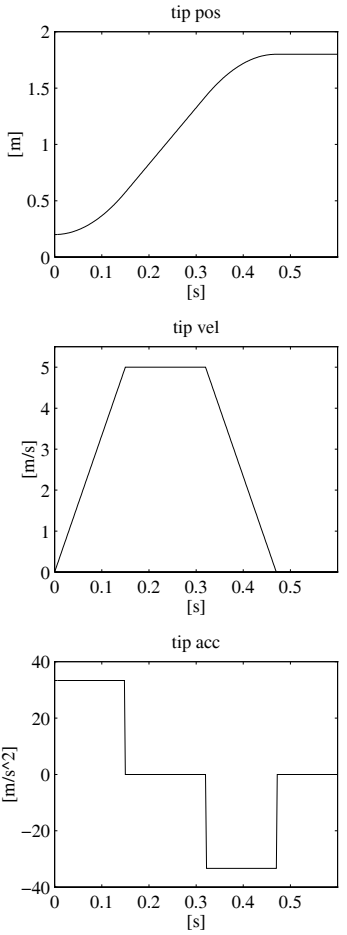

Fig. 7.9. Time history of tip position, velocity and acceleration with a straight line tip trajectory along the horizontal axis

- The inertia torques at each joint due to acceleration of the other joint confirm the symmetry of the inertia matrix, since the acceleration profiles are the same for both joints.
- The Coriolis effect is present only at Joint 1, since the arm tip moves with respect to the mobile frame attached to Link 1 but is fixed with respect to the frame attached to Link 2.
- The centrifugal and Coriolis torques reflect the above symmetry.

Figure 7.7 shows the time history of positions, velocities, accelerations and torques resulting from joint trajectories with typical trapezoidal velocity profile and different time duration. The initial configuration is the same as in the previous case. The two joints make a rotation so as to take the tip to the point $(1.8, 0)$ m. The acceleration time is 0.15 s and the maximum velocity is 5 rad/s for both joints.

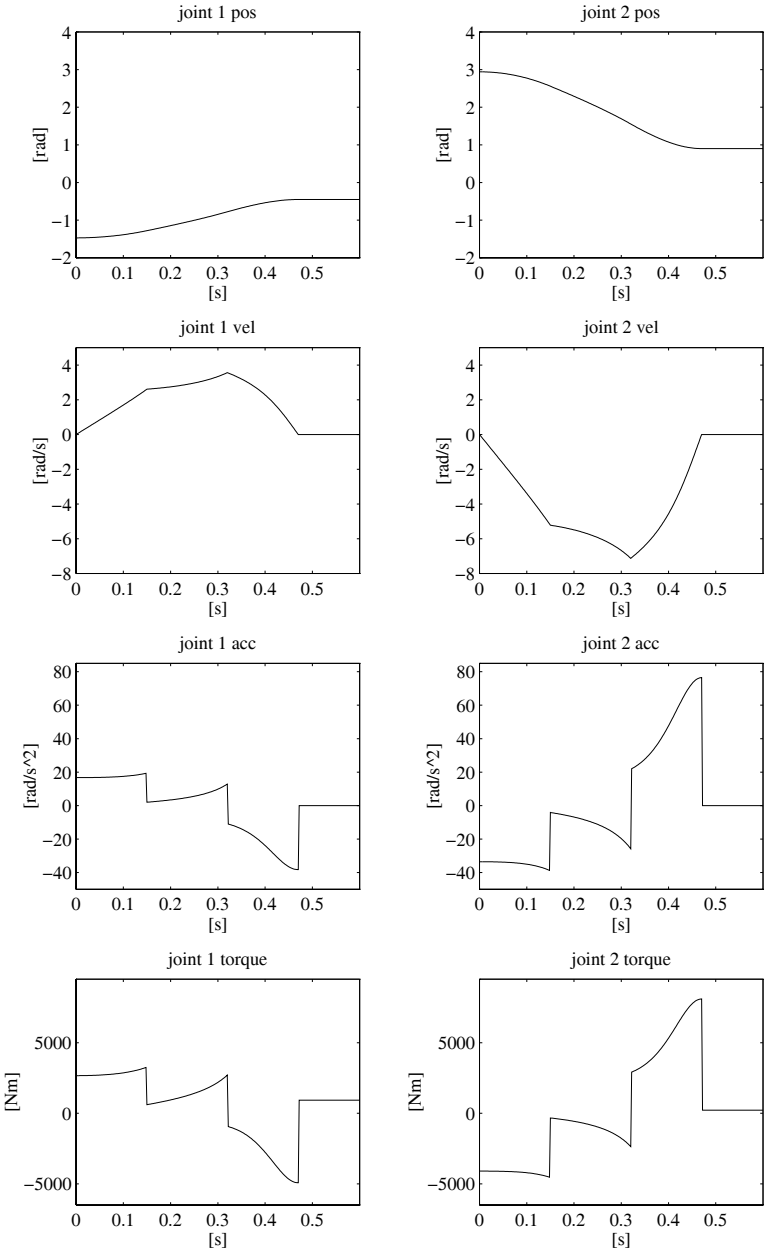

Fig. 7.10. Time history of joint positions, velocities, accelerations, and torques with a straight line tip trajectory along the horizontal axis

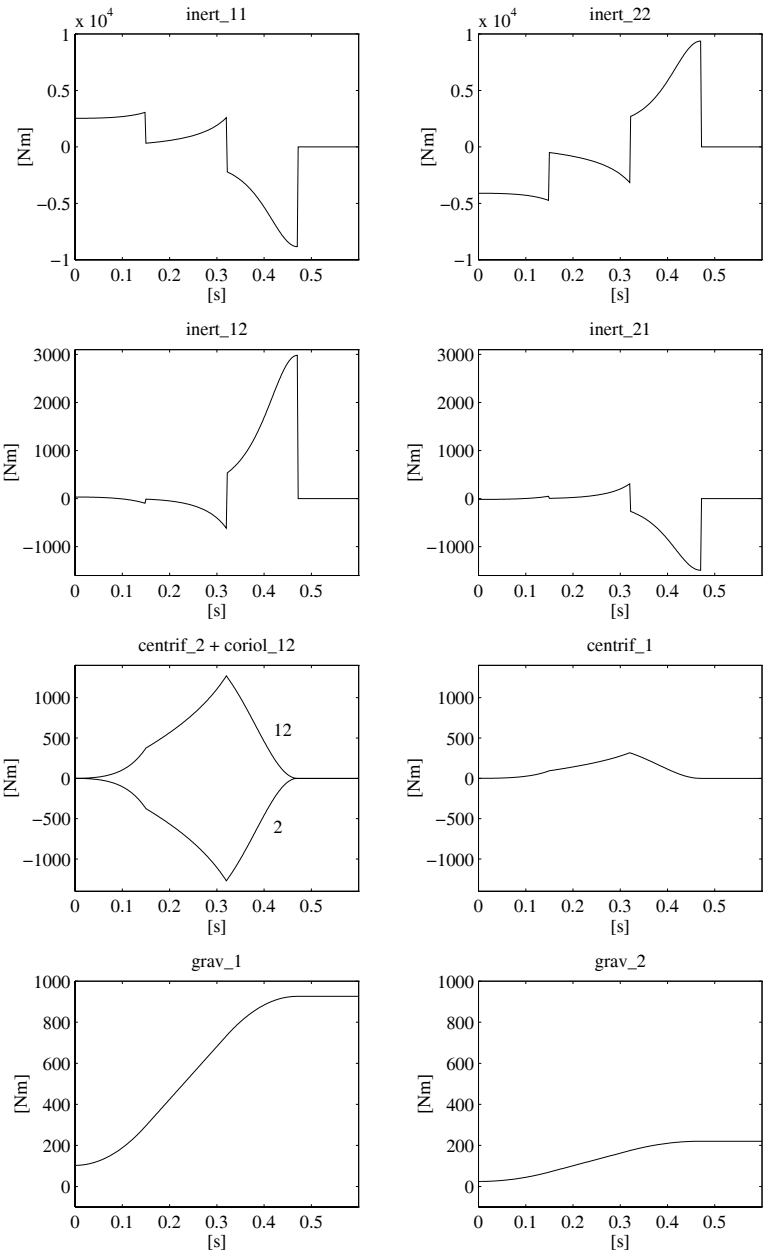

Fig. 7.11. Time history of joint torque contributions with a straight line tip trajectory along the horizontal axis

From the time history of the single torque contributions in Fig. 7.8 it can be recognized that:

- The inertia torque at Joint 1 due to Joint 2 acceleration is opposite to that at Joint 2 due to Joint 1 acceleration in that portion of trajectory when the two accelerations have the same magnitude but opposite sign.
- The different velocity profiles imply that the centrifugal effect induced at Joint 1 by Joint 2 velocity dies out later than the centrifugal effect induced at Joint 2 by Joint 1 velocity.
- The gravitational torque at Joint 2 is practically constant in the first portion of the trajectory, since Link 2 is almost kept in the same posture. As for the gravitational torque at Joint 1, instead, the centre of mass of the articulated system moves away from the origin of the axes.

Finally, Fig. 7.9 shows the time history of tip position, velocity and acceleration for a trajectory with a trapezoidal velocity profile. Starting from the same initial posture as above, the arm tip makes a translation of 1.6 m along the horizontal axis; the acceleration time is 0.15 s and the maximum velocity is 5 m/s.

As a result of an inverse kinematics procedure, the time history of joint positions, velocities and accelerations have been computed which are illustrated in Fig. 7.10, together with the joint torques that are needed to execute the assigned trajectory. It can be noticed that the time history of the represented quantities differs from the corresponding ones in the operational space, in view of the nonlinear effects introduced by kinematic relations.

For what concerns the time history of the individual torque contributions in Fig. 7.11, it is possible to make a number of remarks similar to those made above for trajectories assigned directly in the joint space.

7.3.3 Parallelogram Arm

Consider the parallelogram arm in Fig. 7.12. Because of the presence of the closed chain, the equivalent tree-structured open-chain arm is initially taken into account. Let $\ell_{1'}$, $\ell_{2'}$, $\ell_{3'}$ and $\ell_{1''}$ be the distances of the centres of mass of the three links along one branch of the tree, and of the single link along the other branch, from the respective joint axes. Also let $m_{\ell_{1'}}$, $m_{\ell_{2'}}$, $m_{\ell_{3'}}$ and $m_{\ell_{1''}}$ be the masses of the respective links, and $I_{\ell_{1'}}$, $I_{\ell_{2'}}$, $I_{\ell_{3'}}$ and $I_{\ell_{1''}}$ the moments of inertia relative to the centres of mass of the respective links. For the sake of simplicity, the contributions of the motors are neglected.

With the chosen coordinate frames, computation of the Jacobians in (7.16) (7.18) yields

$$\boldsymbol{J}_P^{(\ell_{1'})} = \begin{bmatrix} -\ell_{1'}s_{1'} & 0 & 0 \\ \ell_{1'}c_{1'} & 0 & 0 \\ 0 & 0 & 0 \end{bmatrix} \qquad \boldsymbol{J}_P^{(\ell_{2'})} = \begin{bmatrix} -a_{1'}s_{1'} - \ell_2 s_{1'2'} & -\ell_{2'}s_{1'2'} & 0 \\ a_{1'}c_{1'} + \ell_{2'}c_{1'2'} & \ell_2 c_{1'2'} & 0 \\ 0 & 0 & 0 \end{bmatrix}$$

$$\boldsymbol{J}_P^{(\ell_{3'})} = \begin{bmatrix} -a_{1'}s_{1'} - a_{2'}s_{1'2'} - \ell_{3'}s_{1'2'3'} & -a_{2'}s_{1'2'} - \ell_{3'}s_{1'2'3'} & -\ell_{3'}s_{1'2'3'} \\ a_{1'}c_{1'} + a_{2'}c_{1'2'} + \ell_{3'}c_{1'2'3'} & a_{2'}c_{1'2'} + \ell_{3'}c_{1'2'3'} & \ell_{3'}c_{1'2'3'} \\ 0 & 0 & 0 \end{bmatrix}$$

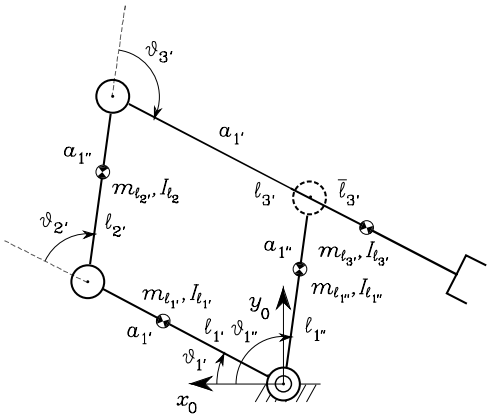

Fig. 7.12. Parallelogram arm

and

$$\boldsymbol{J}_P^{(\ell_{1''})} = \begin{bmatrix} -\ell_{1''} s_{1''} \\ \ell_{1''} c_{1''} \\ 0 \end{bmatrix},$$

whereas computation of the Jacobians in (7.17), (7.19) yields

$$\boldsymbol{J}_O^{(\ell_{1'})} = \begin{bmatrix} 0 & 0 & 0 \\ 0 & 0 & 0 \\ 1 & 0 & 0 \end{bmatrix} \qquad \boldsymbol{J}_O^{(\ell_{2'})} = \begin{bmatrix} 0 & 0 & 0 \\ 0 & 0 & 0 \\ 1 & 1 & 0 \end{bmatrix} \qquad \boldsymbol{J}_O^{(\ell_{3'})} = \begin{bmatrix} 0 & 0 & 0 \\ 0 & 0 & 0 \\ 1 & 1 & 1 \end{bmatrix}$$

and

$$\boldsymbol{J}_O^{(\ell_{1''})} = \begin{bmatrix} 0 \\ 0 \\ 1 \end{bmatrix}.$$

From (7.32), the inertia matrix of the virtual arm composed of joints $\vartheta_{1'}$, $\vartheta_{2'}$, $\vartheta_{3'}$ is

$$\boldsymbol{B}'(\boldsymbol{q}') = \begin{bmatrix} b_{1'1'}(\vartheta_{2'}, \vartheta_{3'}) & b_{1'2'}(\vartheta_{2'}, \vartheta_{3'}) & b_{1'3'}(\vartheta_{2'}, \vartheta_{3'}) \\ b_{2'1'}(\vartheta_{2'}, \vartheta_{3'}) & b_{2'2'}(\vartheta_{3'}) & b_{2'3'}(\vartheta_{3'}) \\ b_{3'1'}(\vartheta_{2'}, \vartheta_{3'}) & b_{3'2'}(\vartheta_{3'}) & b_{3'3'} \end{bmatrix}$$

$$\begin{aligned}
b_{1'1'} &= I_{\ell_{1'}} + m_{\ell_{1'}} \ell_{1'}^2 + I_{\ell_{2'}} + m_{\ell_{2'}} (a_{1'}^2 + \ell_{2'}^2 + 2a_{1'} \ell_{2'} c_{2'}) + I_{\ell_{3'}} \\
&\quad + m_{\ell_{3'}} (a_{1'}^2 + a_{2'}^2 + \ell_{3'}^2 + 2a_{1'} a_{2'} c_{2'} + 2a_{1'} \ell_{3'} c_{2'3'} + 2a_{2'} \ell_{3'} c_{3'}) \\
b_{1'2'} &= b_{2'1'} = I_{\ell_{2'}} + m_{\ell_{2'}} (\ell_{2'}^2 + a_{1'} \ell_{2'} c_{2'}) + I_{\ell_{3'}} \\
&\quad + m_{\ell_{3'}} (a_{2'}^2 + \ell_{3'}^2 + a_{1'} a_{2'} c_{2'} + a_{1'} \ell_{3'} c_{2'3'} + 2a_{2'} \ell_{3'} c_{3'}) \\
b_{1'3'} &= b_{31} = I_{\ell_{3'}} + m_{\ell_{3'}} (\ell_{3'}^2 + a_{1'} \ell_{3'} c_{2'3'} + a_{2'} \ell_{3'} c_{3'}) \\
b_{2'2'} &= I_{\ell_{2'}} + m_{\ell_{2'}} \ell_{2'}^2 + I_{\ell_{3'}} + m_{\ell_{3'}} (a_{2'}^2 + \ell_{3'}^2 + 2a_{2'} \ell_{3'} c_{3'}) \\
b_{2'3'} &= I_{\ell_{3'}} + m_{\ell_{3'}} (\ell_{3'}^2 + a_{2'} \ell_{3'} c_{3'}) \\
b_{3'3'} &= I_{\ell_{3'}} + m_{\ell_{3'}} \ell_{3'}^2
\end{aligned}$$

while the moment of inertia of the virtual arm composed of just joint $\vartheta_{1''}$ is

$$b_{1''1''} = I_{\ell_{1''}} + m_{\ell_{1''}} \ell_{1''}^2.$$

Therefore, the inertial torque contributions of the two virtual arms are respectively:

$$\tau_{i'} = \sum_{j'=1'}^{3'} b_{i'j'} \ddot{\vartheta}_{j'} \qquad \tau_{1''} = b_{1''1''} \ddot{\vartheta}_{1''}.$$

At this point, in view of (2.64) and (3.121), the inertial torque contributions at the actuated joints for the closed-chain arm turn out to be

$$\boldsymbol{\tau}_a = \boldsymbol{B}_a \ddot{\boldsymbol{q}}_a$$

where $\boldsymbol{q}_a = [\, \vartheta_{1'} \quad \vartheta_{1''} \,]^T$, $\boldsymbol{\tau}_a = [\, \tau_{a1} \quad \tau_{a2} \,]^T$ and

$$\boldsymbol{B}_a = \begin{bmatrix} b_{a11} & b_{a12} \\ b_{a21} & b_{a22} \end{bmatrix}$$

$$\begin{aligned} b_{a11} &= I_{\ell_{1'}} + m_{\ell_{1'}} \ell_{1'}^2 + m_{\ell_{2'}} a_{1'}^2 + I_{\ell_{3'}} + m_{\ell_{3'}} \ell_{3'}^2 + m_{\ell_{3'}} a_{1'}^2 \\ &\quad - 2 a_{1'} m_{\ell_{3'}} \ell_{3'} \\ b_{a12} &= b_{a21} = \left(a_{1'} m_{\ell_{2'}} \ell_{2'} + a_{1''} m_{\ell_{3'}} (a_{1'} - \ell_{3'}) \right) \cos\left(\vartheta_{1''} - \vartheta_{1'} \right) \\ b_{a22} &= I_{\ell_{1'}} + m_{\ell_{1'}} \ell_{1'}^2 + I_{\ell_{2'}} + m_{\ell_{2'}} \ell_{2'}^2 + m_{\ell_{3'}} a_{1''}^2. \end{aligned}$$

This expression reveals the possibility of obtaining a *configuration-independent* and *decoupled* inertia matrix; to this end it is sufficient to design the four links of the parallelogram so that

$$\frac{m_{\ell_{3'}} \bar{\ell}_{3'}}{m_{\ell_{2'}} \ell_{2'}} = \frac{a_{1'}}{a_{1''}}$$

where $\bar{\ell}_{3'} = \ell_{3'} - a_{1'}$ is the distance of the centre of mass of Link $3'$ from the axis of Joint 4. If this condition is satisfied, then the inertia matrix is diagonal ($b_{a12} = b_{a21} = 0$) with

$$\begin{aligned} b_{a11} &= I_{\ell_{1'}} + m_{\ell_{1'}} \ell_{1'}^2 + m_{\ell_{2'}} a_{1'}^2 \left(1 + \frac{\ell_{2'} \bar{\ell}_{3'}}{a_{1'} a_{1''}} \right) + I_{\ell_{3'}} \\ b_{a22} &= I_{\ell_{1'}} + m_{\ell_{1'}} \ell_{1'}^2 + I_{\ell_{2'}} + m_{\ell_{2'}} \ell_{2'}^2 \left(1 + \frac{a_{1'} a_{1''}}{\ell_{2'} \bar{\ell}_{3'}} \right). \end{aligned}$$

As a consequence, no contributions of Coriolis and centrifugal torques are obtained. Such a result could not be achieved with the previous two-link planar arm, no matter how the design parameters were chosen.

As for the gravitational terms, since $\boldsymbol{g}_0 = [\,0 \quad -g \quad 0\,]^T$, (7.39) with the above Jacobians gives

$$\begin{aligned} g_{1'} &= (m_{\ell_{1'}}\ell_{1'} + m_{\ell_{2'}}a_{1'} + m_{\ell_{3'}}a_{1'})gc_{1'} + (m_{\ell_{2'}}\ell_{2'} + m_{\ell_{3'}}a_{2'})gc_{1'2'} \\ &\quad + m_{\ell_{3'}}\ell_{3'}gc_{1'2'3} \\ g_{2'} &= (m_{\ell_{2'}}\ell_{2'} + m_{\ell_{3'}}a_{2'})gc_{1'2'} + m_{\ell_{3'}}\ell_{3'}gc_{1'2'3} \\ g_{3'} &= m_{\ell_{3'}}\ell_{3'}gc_{1'2'3} \end{aligned}$$

and

$$g_{1''} = m_{\ell_{1''}}\ell_{1''}gc_{1''}.$$

Composing the various contributions as done above yields

$$\boldsymbol{g}_a = \begin{bmatrix} (m_{\ell_{1'}}\ell_{1'} + m_{\ell_{2'}}a_{1'} - m_{\ell_{3'}}\bar{\ell}_{3'})gc_{1'} \\ (m_{\ell_{1''}}\ell_{1''} + m_{\ell_{2'}}\ell_{2'} + m_{\ell_{3'}}a_{1''})gc_{1''} \end{bmatrix}$$

which, together with the inertial torques, completes the derivation of the sought dynamic model.

A final comment is in order. In spite of its kinematic equivalence with the two-link planar arm, the dynamic model of the parallelogram is remarkably lighter. This property is quite advantageous for trajectory planning and control purposes. For this reason, apart from obvious considerations related to manipulation of heavy payloads, the adoption of closed kinematic chains in the design of industrial robots has received a great deal of attention.

7.4 Dynamic Parameter Identification

The use of the dynamic model for solving simulation and control problems demands the knowledge of the values of dynamic parameters of the manipulator model.

Computing such parameters from the design data of the mechanical structure is not simple. CAD modelling techniques can be adopted which allow the computation of the values of the inertial parameters of the various components (links, actuators and transmissions) on the basis of their geometry and type of materials employed. Nevertheless, the estimates obtained by such techniques are inaccurate because of the simplification typically introduced by geometric modelling; moreover, complex dynamic effects, such as joint friction, cannot be taken into account.

A heuristic approach could be to dismantle the various components of the manipulator and perform a series of measurements to evaluate the inertial parameters. Such technique is not easy to implement and may be troublesome to measure the relevant quantities.

In order to find accurate estimates of dynamic parameters, it is worth resorting to *identification* techniques which conveniently exploit the *property of linearity* (7.81) of the manipulator model with respect to a suitable set of

dynamic parameters. Such techniques allow the computation of the parameter vector $\boldsymbol{\pi}$ from the measurements of joint torques $\boldsymbol{\tau}$ and of relevant quantities for the evaluation of the matrix $\boldsymbol{Y}$, when suitable motion trajectories are imposed to the manipulator.

On the assumption that the kinematic parameters in the matrix $\boldsymbol{Y}$ are known with good accuracy, e.g., as a result of a kinematic calibration, measurements of joint positions $\boldsymbol{q}$, velocities $\dot{\boldsymbol{q}}$ and accelerations $\ddot{\boldsymbol{q}}$ are required. Joint positions and velocities can be actually measured while numerical reconstruction of accelerations is needed; this can be performed on the basis of the position and velocity values recorded during the execution of the trajectories. The reconstructing filter does not work in real time and thus it can also be anti-causal, allowing an accurate reconstruction of the accelerations.

As regards joint torques, in the unusual case of torque sensors at the joint, these can be measured directly. Otherwise, they can be evaluated from either wrist force measurements or current measurements in the case of electric actuators.

If measurements of joint torques, positions, velocities and accelerations have been obtained at given time instants $t_1, \ldots, t_N$ along a given trajectory, one may write

$$\bar{\boldsymbol{\tau}} = \begin{bmatrix} \boldsymbol{\tau}(t_1) \\ \vdots \\ \boldsymbol{\tau}(t_N) \end{bmatrix} = \begin{bmatrix} \boldsymbol{Y}(t_1) \\ \vdots \\ \boldsymbol{Y}(t_N) \end{bmatrix} \boldsymbol{\pi} = \bar{\boldsymbol{Y}} \boldsymbol{\pi}. \tag{7.85}$$

The number of time instants sets the number of measurements to perform and should be large enough (typically $Nn \gg p$) so as to avoid ill-conditioning of matrix $\bar{\boldsymbol{Y}}$. Solving (7.85) by a least-squares technique leads to the solution in the form

$$\boldsymbol{\pi} = (\bar{\boldsymbol{Y}}^T \bar{\boldsymbol{Y}})^{-1} \bar{\boldsymbol{Y}}^T \bar{\boldsymbol{\tau}} \tag{7.86}$$

where $(\bar{\boldsymbol{Y}}^T \bar{\boldsymbol{Y}})^{-1} \bar{\boldsymbol{Y}}^T$ is the *left pseudo-inverse* matrix of $\bar{\boldsymbol{Y}}$.

It should be noticed that, in view of the block triangular structure of matrix $\boldsymbol{Y}$ in (7.80), computation of parameter estimates could be simplified by resorting to a sequential procedure. Take the equation $\tau_n = \boldsymbol{y}_{nn}^T \boldsymbol{\pi}_n$ and solve it for $\boldsymbol{\pi}_n$ by specifying τ_n and $\boldsymbol{y}_{nn}^T$ for a given trajectory on Joint n. By iterating the procedure, the manipulator parameters can be identified on the basis of measurements performed joint by joint from the outer link to the base. Such procedure, however, may have the inconvenience to accumulate any error due to ill-conditioning of the matrices involved step by step. It may then be worth operating with a global procedure by imposing motions on all manipulator joints at the same time.

Regarding the rank of matrix $\bar{\boldsymbol{Y}}$, it is possible to identify only the dynamic parameters of the manipulator that contribute to the dynamic model. Example 7.2 has indeed shown that for the two-link planar arm considered, only 8 out of the 22 possible dynamic parameters appear in the dynamic model. Hence, there exist some dynamic parameters which, in view of the disposition

of manipulator links and joints, are *non-identifiable*, since for any trajectory assigned to the structure they do not contribute to the equations of motion. A direct consequence is that the columns of the matrix $\boldsymbol{Y}$ in (7.80) corresponding to such parameters are null and thus they have to be removed from the matrix itself; e.g., the resulting (2×8) matrix in (7.84).

Another issue to consider about determination of the effective number of parameters that can be identified by (7.86) is that some parameters can be *identified in linear combinations* whenever they do not appear isolated in the equations. In such a case, it is necessary, for each linear combination, to remove as many columns of the matrix $\boldsymbol{Y}$ as the number of parameters in the linear combination minus one.

For the determination of the minimum number of identifiable parameters that allow direct application of the least-squares technique based on (7.86), it is possible to inspect directly the equations of the dynamic model, as long as the manipulator has few joints. Otherwise, numerical techniques based on singular value decomposition of matrix $\bar{\boldsymbol{Y}}$ have to be used. If the matrix $\bar{\boldsymbol{Y}}$ resulting from a series of measurements is not full-rank, one has to resort to a *damped least-squares inverse* of $\bar{\boldsymbol{Y}}$ where solution accuracy depends on the weight of the damping factor.

In the above discussion, the type of trajectory imposed to the manipulator joints has not been explicitly addressed. It can be generally ascertained that the choice should be oriented in favor of polynomial type trajectories which are sufficiently *rich* to allow an accurate evaluation of the identifiable parameters. This corresponds to achieving a low condition number of the matrix $\bar{\boldsymbol{Y}}^T \bar{\boldsymbol{Y}}$ along the trajectory. On the other hand, such trajectories should not excite any unmodelled dynamic effects such as joint elasticity or link flexibility that would naturally lead to unreliable estimates of the dynamic parameters to identify.

Finally, it is worth observing that the technique presented above can also be extended to the identification of the dynamic parameters of an unknown payload at the manipulator's end-effector. In such a case, the payload can be regarded as a structural modification of the last link and one may proceed to identify the dynamic parameters of the modified link. To this end, if a force sensor is available at the manipulator's wrist, it is possible to characterize directly the dynamic parameters of the payload starting from force sensor measurements.

7.5 Newton–Euler Formulation

In the Lagrange formulation, the manipulator dynamic model is derived starting from the total Lagrangian of the system. On the other hand, the *Newton–Euler* formulation is based on a balance of all the forces acting on the generic link of the manipulator. This leads to a set of equations whose structure allows a recursive type of solution; a forward recursion is performed for propagating

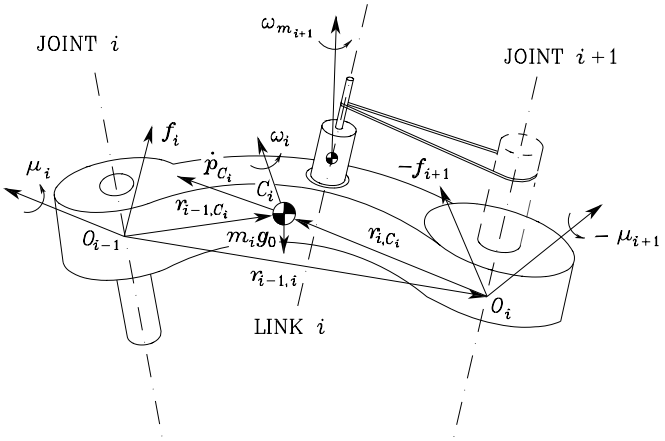

Fig. 7.13. Characterization of Link i for Newton–Euler formulation

link velocities and accelerations, followed by a backward recursion for propagating forces.

Consider the generic *augmented Link i* (Link i plus motor of Joint $i+1$) of the manipulator kinematic chain (Fig. 7.13). According to what was presented in Sect. 7.2.2, one can refer to the centre of mass C_i of the augmented link to characterize the following parameters:

- m_i mass of augmented link,
- $\bar{\boldsymbol{I}}_i$ inertia tensor of augmented link,
- I_{m_i} moment of inertia of rotor,
- $\boldsymbol{r}_{i-1,C_i}$ vector from origin of Frame $(i-1)$ to centre of mass C_i,
- $\boldsymbol{r}_{i,C_i}$ vector from origin of Frame i to centre of mass C_i,
- $\boldsymbol{r}_{i-1,i}$ vector from origin of Frame $(i-1)$ to origin of Frame i.

The velocities and accelerations to be considered are:

- $\dot{\boldsymbol{p}}_{C_i}$ linear velocity of centre of mass C_i,
- $\dot{\boldsymbol{p}}_i$ linear velocity of origin of Frame i,
- $\boldsymbol{\omega}_i$ angular velocity of link,
- $\boldsymbol{\omega}_{m_i}$ angular velocity of rotor,
- $\ddot{\boldsymbol{p}}_{C_i}$ linear acceleration of centre of mass C_i,
- $\ddot{\boldsymbol{p}}_i$ linear acceleration of origin of Frame i,
- $\dot{\boldsymbol{\omega}}_i$ angular acceleration of link,
- $\dot{\boldsymbol{\omega}}_{m_i}$ angular acceleration of rotor,
- $\boldsymbol{g}_0$ gravity acceleration.

The forces and moments to be considered are:

- $\boldsymbol{f}_i$ force exerted by Link $i-1$ on Link i,
- $-\boldsymbol{f}_{i+1}$ force exerted by Link $i+1$ on Link i,

- $\boldsymbol{\mu}_i$ moment exerted by Link $i-1$ on Link i with respect to origin of Frame $i-1$,
- $-\boldsymbol{\mu}_{i+1}$ moment exerted by Link $i+1$ on Link i with respect to origin of Frame i.

Initially, all the vectors and matrices are assumed to be expressed with reference to the *base frame*.

As already anticipated, the Newton–Euler formulation describes the motion of the link in terms of a balance of forces and moments acting on it.

The *Newton* equation for the *translational* motion of the centre of mass can be written as

$$\boldsymbol{f}_i - \boldsymbol{f}_{i+1} + m_i \boldsymbol{g}_0 = m_i \ddot{\boldsymbol{p}}_{C_i}. \tag{7.87}$$

The *Euler* equation for the *rotational* motion of the link (referring moments to the centre of mass) can be written as

$$\boldsymbol{\mu}_i + \boldsymbol{f}_i \times \boldsymbol{r}_{i-1,C_i} - \boldsymbol{\mu}_{i+1} - \boldsymbol{f}_{i+1} \times \boldsymbol{r}_{i,C_i} = \frac{d}{dt}(\bar{\boldsymbol{I}}_i \boldsymbol{\omega}_i + k_{r,i+1} \dot{q}_{i+1} I_{m_{i+1}} \boldsymbol{z}_{m_{i+1}}), \tag{7.88}$$

where (7.67) has been used for the angular momentum of the rotor. Notice that the gravitational force $m_i \boldsymbol{g}_0$ does not generate any moment, since it is concentrated at the centre of mass.

As pointed out in the above Lagrange formulation, it is convenient to express the inertia tensor in the current frame (constant tensor). Hence, according to (7.12), one has $\bar{\boldsymbol{I}}_i = \boldsymbol{R}_i \bar{\boldsymbol{I}}_i^i \boldsymbol{R}_i^T$, where $\boldsymbol{R}_i$ is the rotation matrix from Frame i to the base frame. Substituting this relation in the first term on the right-hand side of (7.88) yields

$$\begin{aligned} \frac{d}{dt}(\bar{\boldsymbol{I}}_i \boldsymbol{\omega}_i) &= \dot{\boldsymbol{R}}_i \bar{\boldsymbol{I}}_i^i \boldsymbol{R}_i^T \boldsymbol{\omega}_i + \boldsymbol{R}_i \bar{\boldsymbol{I}}_i^i \dot{\boldsymbol{R}}_i^T \boldsymbol{\omega}_i + \boldsymbol{R}_i \bar{\boldsymbol{I}}_i^i \boldsymbol{R}_i^T \dot{\boldsymbol{\omega}}_i \\ &= \boldsymbol{S}(\boldsymbol{\omega}_i) \boldsymbol{R}_i \bar{\boldsymbol{I}}_i^i \boldsymbol{R}_i^T \boldsymbol{\omega}_i + \boldsymbol{R}_i \bar{\boldsymbol{I}}_i^i \boldsymbol{R}_i^T \boldsymbol{S}^T(\boldsymbol{\omega}_i) \boldsymbol{\omega}_i + \boldsymbol{R}_i \bar{\boldsymbol{I}}_i^i \boldsymbol{R}_i^T \dot{\boldsymbol{\omega}}_i \\ &= \bar{\boldsymbol{I}}_i \dot{\boldsymbol{\omega}}_i + \boldsymbol{\omega}_i \times (\bar{\boldsymbol{I}}_i \boldsymbol{\omega}_i) \end{aligned} \tag{7.89}$$

where the second term represents the *gyroscopic* torque induced by the dependence of $\bar{\boldsymbol{I}}_i$ on link orientation.[7] Moreover, by observing that the unit vector $\boldsymbol{z}_{m_{i+1}}$ rotates accordingly to Link i, the derivative needed in the second term on the right-hand side of (7.88) is

$$\frac{d}{dt}(\dot{q}_{i+1} I_{m_{i+1}} \boldsymbol{z}_{m_{i+1}}) = \ddot{q}_{i+1} I_{m_{i+1}} \boldsymbol{z}_{m_{i+1}} + \dot{q}_{i+1} I_{m_{i+1}} \boldsymbol{\omega}_i \times \boldsymbol{z}_{m_{i+1}} \tag{7.90}$$

By substituting (7.89), (7.90) in (7.88), the resulting Euler equation is

$$\begin{aligned} \boldsymbol{\mu}_i + \boldsymbol{f}_i \times \boldsymbol{r}_{i-1,C_i} \; & -\boldsymbol{\mu}_{i+1} - \boldsymbol{f}_{i+1} \times \boldsymbol{r}_{i,C_i} = \bar{\boldsymbol{I}}_i \dot{\boldsymbol{\omega}}_i + \boldsymbol{\omega}_i \times (\bar{\boldsymbol{I}}_i \boldsymbol{\omega}_i) \\ & + k_{r,i+1} \ddot{q}_{i+1} I_{m_{i+1}} \boldsymbol{z}_{m_{i+1}} + k_{r,i+1} \dot{q}_{i+1} I_{m_{i+1}} \boldsymbol{\omega}_i \times \boldsymbol{z}_{m_{i+1}}. \end{aligned} \tag{7.91}$$

[7] In deriving (7.89), the operator $\boldsymbol{S}$ has been introduced to compute the derivative of $\boldsymbol{R}_i$, as in (3.8); also, the property $\boldsymbol{S}^T(\boldsymbol{\omega}_i)\boldsymbol{\omega}_i = \boldsymbol{0}$ has been utilized.

The generalized force at Joint i can be computed by projecting the force $\boldsymbol{f}_i$ for a prismatic joint, or the moment $\boldsymbol{\mu}_i$ for a revolute joint, along the joint axis. In addition, there is the contribution of the rotor inertia torque $k_{ri} I_{m_i} \dot{\boldsymbol{\omega}}_{m_i}^T \boldsymbol{z}_{m_i}$. Hence, the generalized force at Joint i is expressed by

$$\tau_i = \begin{cases} \boldsymbol{f}_i^T \boldsymbol{z}_{i-1} + k_{ri} I_{m_i} \dot{\boldsymbol{\omega}}_{m_i}^T \boldsymbol{z}_{m_i} & \text{for a } \textit{prismatic} \text{ joint} \\ \boldsymbol{\mu}_i^T \boldsymbol{z}_{i-1} + k_{ri} I_{m_i} \dot{\boldsymbol{\omega}}_{m_i}^T \boldsymbol{z}_{m_i} & \text{for a } \textit{revolute} \text{ joint.} \end{cases} \tag{7.92}$$

7.5.1 Link Accelerations

The Newton–Euler equations in (7.87), (7.91) and the equation in (7.92) require the computation of linear and angular acceleration of Link i and Rotor i. This computation can be carried out on the basis of the relations expressing the linear and angular velocities previously derived. The equations in (3.21), (3.22), (3.25), (3.26) can be briefly rewritten as

$$\boldsymbol{\omega}_i = \begin{cases} \boldsymbol{\omega}_{i-1} & \text{for a } \textit{prismatic} \text{ joint} \\ \boldsymbol{\omega}_{i-1} + \dot{\vartheta}_i \boldsymbol{z}_{i-1} & \text{for a } \textit{revolute} \text{ joint} \end{cases} \tag{7.93}$$

and

$$\dot{\boldsymbol{p}}_i = \begin{cases} \dot{\boldsymbol{p}}_{i-1} + \dot{d}_i \boldsymbol{z}_{i-1} + \boldsymbol{\omega}_i \times \boldsymbol{r}_{i-1,i} & \text{for a } \textit{prismatic} \text{ joint} \\ \dot{\boldsymbol{p}}_{i-1} + \boldsymbol{\omega}_i \times \boldsymbol{r}_{i-1,i} & \text{for a } \textit{revolute} \text{ joint.} \end{cases} \tag{7.94}$$

As for the angular acceleration of the link, it can be seen that, for a prismatic joint, differentiating (3.21) with respect to time gives

$$\dot{\boldsymbol{\omega}}_i = \dot{\boldsymbol{\omega}}_{i-1}, \tag{7.95}$$

whereas, for a revolute joint, differentiating (3.25) with respect to time gives

$$\dot{\boldsymbol{\omega}}_i = \dot{\boldsymbol{\omega}}_{i-1} + \ddot{\vartheta}_i \boldsymbol{z}_{i-1} + \dot{\vartheta}_i \boldsymbol{\omega}_{i-1} \times \boldsymbol{z}_{i-1}. \tag{7.96}$$

As for the linear acceleration of the link, for a prismatic joint, differentiating (3.22) with respect to time gives

$$\begin{aligned} \ddot{\boldsymbol{p}}_i = \ddot{\boldsymbol{p}}_{i-1} + \ddot{d}_i \boldsymbol{z}_{i-1} + \dot{d}_i \boldsymbol{\omega}_{i-1} \times \boldsymbol{z}_{i-1} + \dot{\boldsymbol{\omega}}_i \times \boldsymbol{r}_{i-1,i} \\ + \boldsymbol{\omega}_i \times \dot{d}_i \boldsymbol{z}_{i-1} + \boldsymbol{\omega}_i \times (\boldsymbol{\omega}_{i-1} \times \boldsymbol{r}_{i-1,i}) \end{aligned} \tag{7.97}$$

where the relation $\dot{\boldsymbol{r}}_{i-1,i} = \dot{d}_i \boldsymbol{z}_{i-1} + \boldsymbol{\omega}_{i-1} \times \boldsymbol{r}_{i-1,i}$ has been used. Hence, in view of (3.21), the equation in (7.97) can be rewritten as

$$\ddot{\boldsymbol{p}}_i = \ddot{\boldsymbol{p}}_{i-1} + \ddot{d}_i \boldsymbol{z}_{i-1} + 2\dot{d}_i \boldsymbol{\omega}_i \times \boldsymbol{z}_{i-1} + \dot{\boldsymbol{\omega}}_i \times \boldsymbol{r}_{i-1,i} + \boldsymbol{\omega}_i \times (\boldsymbol{\omega}_i \times \boldsymbol{r}_{i-1,i}). \tag{7.98}$$

Also, for a revolute joint, differentiating (3.26) with respect to time gives

$$\ddot{\boldsymbol{p}}_i = \ddot{\boldsymbol{p}}_{i-1} + \dot{\boldsymbol{\omega}}_i \times \boldsymbol{r}_{i-1,i} + \boldsymbol{\omega}_i \times (\boldsymbol{\omega}_i \times \boldsymbol{r}_{i-1,i}). \tag{7.99}$$

In summary, the equations in (7.95), (7.96), (7.98), (7.99) can be compactly rewritten as

$$\dot{\boldsymbol{\omega}}_i = \begin{cases} \dot{\boldsymbol{\omega}}_{i-1} & \text{for a } \textit{prismatic} \text{ joint} \\ \dot{\boldsymbol{\omega}}_{i-1} + \ddot{\vartheta}_i \boldsymbol{z}_{i-1} + \dot{\vartheta}_i \boldsymbol{\omega}_{i-1} \times \boldsymbol{z}_{i-1} & \text{for a } \textit{revolute} \text{ joint} \end{cases} \tag{7.100}$$

and

$$\ddot{\boldsymbol{p}}_i = \begin{cases} \ddot{\boldsymbol{p}}_{i-1} + \ddot{d}_i \boldsymbol{z}_{i-1} + 2\dot{d}_i \boldsymbol{\omega}_i \times \boldsymbol{z}_{i-1} & \text{for a } \textit{prismatic} \text{ joint} \\ \quad + \dot{\boldsymbol{\omega}}_i \times \boldsymbol{r}_{i-1,i} + \boldsymbol{\omega}_i \times (\boldsymbol{\omega}_i \times \boldsymbol{r}_{i-1,i}) & \\ \ddot{\boldsymbol{p}}_{i-1} + \dot{\boldsymbol{\omega}}_i \times \boldsymbol{r}_{i-1,i} & \text{for a } \textit{revolute} \text{ joint.} \\ \quad + \boldsymbol{\omega}_i \times (\boldsymbol{\omega}_i \times \boldsymbol{r}_{i-1,i}) & \end{cases} \tag{7.101}$$

The acceleration of the centre of mass of Link i required by the Newton equation in (7.87) can be derived from (3.15), since $\dot{\boldsymbol{r}}^i_{i,C_i} = \boldsymbol{0}$; by differentiating (3.15) with respect to time, the acceleration of the centre of mass C_i can be expressed as a function of the velocity and acceleration of the origin of Frame i, i.e.,

$$\ddot{\boldsymbol{p}}_{C_i} = \ddot{\boldsymbol{p}}_i + \dot{\boldsymbol{\omega}}_i \times \boldsymbol{r}_{i,C_i} + \boldsymbol{\omega}_i \times (\boldsymbol{\omega}_i \times \boldsymbol{r}_{i,C_i}). \tag{7.102}$$

Finally, the angular acceleration of the rotor can be obtained by time differentiation of (7.23), i.e.,

$$\dot{\boldsymbol{\omega}}_{m_i} = \dot{\boldsymbol{\omega}}_{i-1} + k_{ri} \ddot{q}_i \boldsymbol{z}_{m_i} + k_{ri} \dot{q}_i \boldsymbol{\omega}_{i-1} \times \boldsymbol{z}_{m_i}. \tag{7.103}$$

7.5.2 Recursive Algorithm

It is worth remarking that the resulting Newton–Euler equations of motion are *not* in *closed form*, since the motion of a single link is coupled to the motion of the other links through the kinematic relationship for velocities and accelerations.

Once the joint positions, velocities and accelerations are known, one can compute the link velocities and accelerations, and the Newton–Euler equations can be utilized to find the forces and moments acting on each link in a recursive fashion, starting from the force and moment applied to the end-effector. On the other hand, also link and rotor velocities and accelerations can be computed recursively starting from the velocity and acceleration of the base link. In summary, a computationally *recursive algorithm* can be constructed that features a *forward recursion* relative to the propagation of *velocities and accelerations* and a *backward recursion* for the propagation of *forces and moments* along the structure.

For the forward recursion, once $\boldsymbol{q}$, $\dot{\boldsymbol{q}}$, $\ddot{\boldsymbol{q}}$, and the velocity and acceleration of the base link $\boldsymbol{\omega}_0$, $\ddot{\boldsymbol{p}}_0 - \boldsymbol{g}_0$, $\dot{\boldsymbol{\omega}}_0$ are specified, $\boldsymbol{\omega}_i$, $\dot{\boldsymbol{\omega}}_i$, $\ddot{\boldsymbol{p}}_i$, $\ddot{\boldsymbol{p}}_{C_i}$, $\dot{\boldsymbol{\omega}}_{m_i}$ can be computed using (7.93), (7.100), (7.101), (7.102), (7.103), respectively. Notice that the linear acceleration has been taken as $\ddot{\boldsymbol{p}}_0 - \boldsymbol{g}_0$ so as to incorporate the

term $-\boldsymbol{g}_0$ in the computation of the acceleration of the centre of mass $\ddot{\boldsymbol{p}}_{C_i}$ via (7.101), (7.102).

Having computed the velocities and accelerations with the forward recursion from the base link to the end-effector, a backward recursion can be carried out for the forces. In detail, once $\boldsymbol{h}_e = [\, \boldsymbol{f}_{n+1}^T \quad \boldsymbol{\mu}_{n+1}^T \,]^T$ is given (eventually $\boldsymbol{h}_e = \boldsymbol{0}$), the Newton equation in (7.87) to be used for the recursion can be rewritten as

$$\boldsymbol{f}_i = \boldsymbol{f}_{i+1} + m_i \ddot{\boldsymbol{p}}_{C_i} \tag{7.104}$$

since the contribution of gravity acceleration has already been included in $\ddot{\boldsymbol{p}}_{C_i}$. Further, the Euler equation gives

$$\begin{aligned} \boldsymbol{\mu}_i = &-\boldsymbol{f}_i \times (\boldsymbol{r}_{i-1,i} + \boldsymbol{r}_{i,C_i}) + \boldsymbol{\mu}_{i+1} + \boldsymbol{f}_{i+1} \times \boldsymbol{r}_{i,C_i} + \bar{\boldsymbol{I}}_i \dot{\boldsymbol{\omega}}_i + \boldsymbol{\omega}_i \times (\bar{\boldsymbol{I}}_i \boldsymbol{\omega}_i) \\ &+ k_{r,i+1} \ddot{q}_{i+1} I_{m_{i+1}} \boldsymbol{z}_{m_{i+1}} + k_{r,i+1} \dot{q}_{i+1} I_{m_{i+1}} \boldsymbol{\omega}_i \times \boldsymbol{z}_{m_{i+1}} \end{aligned} \tag{7.105}$$

which derives from (7.91), where $\boldsymbol{r}_{i-1,C_i}$ has been expressed as the sum of the two vectors appearing already in the forward recursion. Finally, the generalized forces resulting at the joints can be computed from (7.92) as

$$\tau_i = \begin{cases} \boldsymbol{f}_i^T \boldsymbol{z}_{i-1} + k_{ri} I_{m_i} \dot{\boldsymbol{\omega}}_{m_i}^T \boldsymbol{z}_{m_i} & \\ \quad + F_{vi} \dot{d}_i + F_{si} \operatorname{sgn}(\dot{d}_i) & \text{for a } \textit{prismatic} \text{ joint} \\ \boldsymbol{\mu}_i^T \boldsymbol{z}_{i-1} + k_{ri} I_{m_i} \dot{\boldsymbol{\omega}}_{m_i}^T \boldsymbol{z}_{m_i} & \\ \quad + F_{vi} \dot{\vartheta}_i + F_{si} \operatorname{sgn}(\dot{\vartheta}_i) & \text{for a } \textit{revolute} \text{ joint,} \end{cases} \tag{7.106}$$

where joint viscous and Coulomb friction torques have been included.

In the above derivation, it has been assumed that all vectors were referred to the base frame. To simplify greatly computation, however, the recursion is computationally more efficient if all vectors are referred to the current frame on Link i. This implies that all vectors that need to be transformed from Frame $i+1$ into Frame i have to be multiplied by the rotation matrix $\boldsymbol{R}_{i+1}^i$, whereas all vectors that need to be transformed from Frame $i-1$ into Frame i have to be multiplied by the rotation matrix $\boldsymbol{R}_i^{i-1T}$. Therefore, the equations in (7.93), (7.100), (7.101), (7.102), (7.103), (7.104), (7.105), (7.106) can be rewritten as:

$$\boldsymbol{\omega}_i^i = \begin{cases} \boldsymbol{R}_i^{i-1T} \boldsymbol{\omega}_{i-1}^{i-1} & \text{for a } \textit{prismatic} \text{ joint} \\ \boldsymbol{R}_i^{i-1T} (\boldsymbol{\omega}_{i-1}^{i-1} + \dot{\vartheta}_i \boldsymbol{z}_0) & \text{for a } \textit{revolute} \text{ joint} \end{cases} \tag{7.107}$$

$$\dot{\boldsymbol{\omega}}_i^i = \begin{cases} \boldsymbol{R}_i^{i-1T} \dot{\boldsymbol{\omega}}_{i-1}^{i-1} & \text{for a } \textit{prismatic} \text{ joint} \\ \boldsymbol{R}_i^{i-1T} (\dot{\boldsymbol{\omega}}_{i-1}^{i-1} + \ddot{\vartheta}_i \boldsymbol{z}_0 + \dot{\vartheta}_i \boldsymbol{\omega}_{i-1}^{i-1} \times \boldsymbol{z}_0) & \text{for a } \textit{revolute} \text{ joint} \end{cases} \tag{7.108}$$

$$\ddot{\boldsymbol{p}}_i^i = \begin{cases} \boldsymbol{R}_i^{i-1T} (\ddot{\boldsymbol{p}}_{i-1}^{i-1} + \ddot{d}_i \boldsymbol{z}_0) + 2 \dot{d}_i \boldsymbol{\omega}_i^i \times \boldsymbol{R}_i^{i-1T} \boldsymbol{z}_0 & \\ \quad + \dot{\boldsymbol{\omega}}_i^i \times \boldsymbol{r}_{i-1,i}^i + \boldsymbol{\omega}_i^i \times (\boldsymbol{\omega}_i^i \times \boldsymbol{r}_{i-1,i}^i) & \text{for a } \textit{prismatic} \text{ joint} \\ \boldsymbol{R}_i^{i-1T} \ddot{\boldsymbol{p}}_{i-1}^{i-1} + \dot{\boldsymbol{\omega}}_i^i \times \boldsymbol{r}_{i-1,i}^i & \\ \quad + \boldsymbol{\omega}_i^i \times (\boldsymbol{\omega}_i^i \times \boldsymbol{r}_{i-1,i}^i) & \text{for a } \textit{revolute} \text{ joint} \end{cases} \tag{7.109}$$

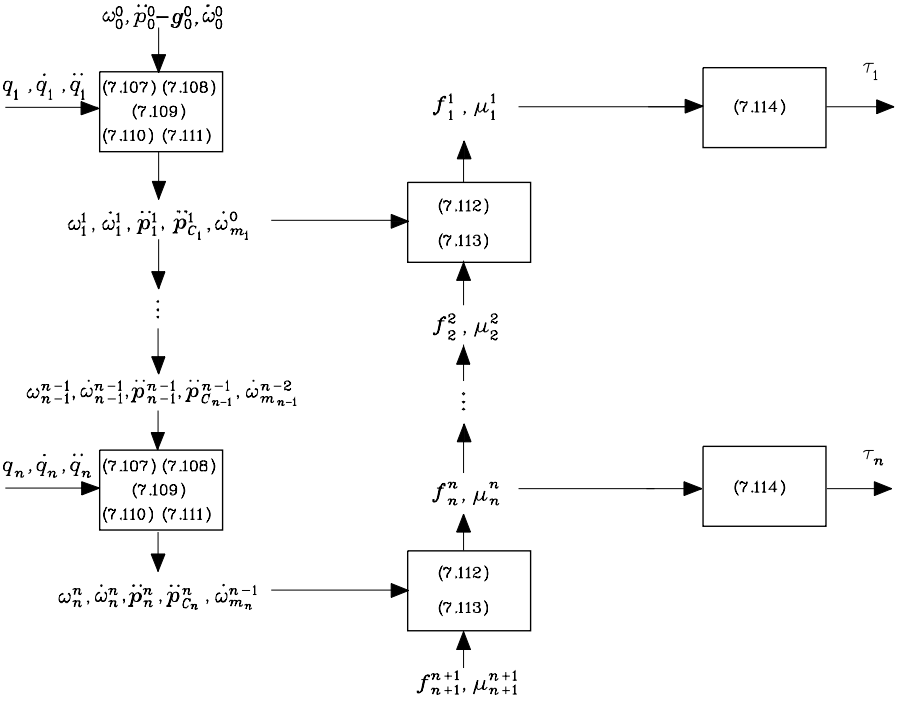

Fig. 7.14. Computational structure of the Newton–Euler recursive algorithm

$$\ddot{\boldsymbol{p}}^i_{C_i} = \ddot{\boldsymbol{p}}^i_i + \dot{\boldsymbol{\omega}}^i_i \times \boldsymbol{r}^i_{i,C_i} + \boldsymbol{\omega}^i_i \times (\boldsymbol{\omega}^i_i \times \boldsymbol{r}^i_{i,C_i}) \tag{7.110}$$

$$\dot{\boldsymbol{\omega}}^{i-1}_{m_i} = \dot{\boldsymbol{\omega}}^{i-1}_{i-1} + k_{ri}\ddot{q}_i \boldsymbol{z}^{i-1}_{m_i} + k_{ri}\dot{q}_i \boldsymbol{\omega}^{i-1}_{i-1} \times \boldsymbol{z}^{i-1}_{m_i} \tag{7.111}$$

$$\boldsymbol{f}^i_i = \boldsymbol{R}^i_{i+1}\boldsymbol{f}^{i+1}_{i+1} + m_i \ddot{\boldsymbol{p}}^i_{C_i} \tag{7.112}$$

$$\begin{aligned}\boldsymbol{\mu}^i_i = {} & -\boldsymbol{f}^i_i \times (\boldsymbol{r}^i_{i-1,i} + \boldsymbol{r}^i_{i,C_i}) + \boldsymbol{R}^i_{i+1}\boldsymbol{\mu}^{i+1}_{i+1} + \boldsymbol{R}^i_{i+1}\boldsymbol{f}^{i+1}_{i+1} \times \boldsymbol{r}^i_{i,C_i} \\ & + \bar{\boldsymbol{I}}^i_i \dot{\boldsymbol{\omega}}^i_i + \boldsymbol{\omega}^i_i \times (\bar{\boldsymbol{I}}^i_i \boldsymbol{\omega}^i_i) \\ & + k_{r,i+1}\ddot{q}_{i+1} I_{m_{i+1}} \boldsymbol{z}^i_{m_{i+1}} + k_{r,i+1}\dot{q}_{i+1} I_{m_{i+1}} \boldsymbol{\omega}^i_i \times \boldsymbol{z}^i_{m_{i+1}}\end{aligned} \tag{7.113}$$

$$\tau_i = \begin{cases} \boldsymbol{f}^{iT}_i \boldsymbol{R}^{i-1T}_i \boldsymbol{z}_0 + k_{ri} I_{m_i} \dot{\boldsymbol{\omega}}^{i-1T}_{m_i} \boldsymbol{z}^{i-1}_{m_i} \\ \quad + F_{vi}\dot{d}_i + F_{si}\,\mathrm{sgn}\,(\dot{d}_i) & \text{for a } \textit{prismatic} \text{ joint} \\ \boldsymbol{\mu}^{iT}_i \boldsymbol{R}^{i-1T}_i \boldsymbol{z}_0 + k_{ri} I_{m_i} \dot{\boldsymbol{\omega}}^{i-1T}_{m_i} \boldsymbol{z}^{i-1}_{m_i} \\ \quad + F_{vi}\dot{\vartheta}_i + F_{si}\,\mathrm{sgn}\,(\dot{\vartheta}_i) & \text{for a } \textit{revolute} \text{ joint.} \end{cases} \tag{7.114}$$

The above equations have the advantage that the quantities $\bar{\boldsymbol{I}}^i_i$, $\boldsymbol{r}^i_{i,C_i}$, $\boldsymbol{z}^{i-1}_{m_i}$ are *constant*; further, it is $\boldsymbol{z}_0 = [\,0 \quad 0 \quad 1\,]^T$.

To summarize, for given joint positions, velocities and accelerations, the recursive algorithm is carried out in the following two phases:

- With known initial conditions $\boldsymbol{\omega}_0^0$, $\ddot{\boldsymbol{p}}_0^0 - \boldsymbol{g}_0^0$, and $\dot{\boldsymbol{\omega}}_0^0$, use (7.107), (7.108), (7.109), (7.110), (7.111), for $i = 1, \ldots, n$, to compute $\boldsymbol{\omega}_i^i$, $\dot{\boldsymbol{\omega}}_i^i$, $\ddot{\boldsymbol{p}}_i^i$, $\ddot{\boldsymbol{p}}_{C_i}^i$, $\dot{\boldsymbol{\omega}}_{m_i}^{i-1}$.
- With known terminal conditions $\boldsymbol{f}_{n+1}^{n+1}$ and $\boldsymbol{\mu}_{n+1}^{n+1}$, use (7.112), (7.113), for $i = n, \ldots, 1$, to compute $\boldsymbol{f}_i^i$, $\boldsymbol{\mu}_i^i$, and then (7.114) to compute τ_i.

The computational structure of the algorithm is schematically illustrated in Fig. 7.14.

7.5.3 Example

In the following, an example to illustrate the single steps of the Newton–Euler algorithm is developed. Consider the two-link planar arm whose dynamic model has already been derived in Example 7.2.

Start by imposing the initial conditions for the velocities and accelerations:

$$\ddot{\boldsymbol{p}}_0^0 - \boldsymbol{g}_0^0 = [\,0 \quad g \quad 0\,]^T \qquad \boldsymbol{\omega}_0^0 = \dot{\boldsymbol{\omega}}_0^0 = \boldsymbol{0},$$

and the terminal conditions for the forces:

$$\boldsymbol{f}_3^3 = \boldsymbol{0} \qquad \boldsymbol{\mu}_3^3 = \boldsymbol{0}.$$

All quantities are referred to the current link frame. As a consequence, the following constant vectors are obtained:

$$\boldsymbol{r}_{1,C_1}^1 = \begin{bmatrix} \ell_{C_1} \\ 0 \\ 0 \end{bmatrix} \quad \boldsymbol{r}_{0,1}^1 = \begin{bmatrix} a_1 \\ 0 \\ 0 \end{bmatrix} \quad \boldsymbol{r}_{2,C_2}^2 = \begin{bmatrix} \ell_{C_2} \\ 0 \\ 0 \end{bmatrix} \quad \boldsymbol{r}_{1,2}^2 = \begin{bmatrix} a_2 \\ 0 \\ 0 \end{bmatrix}$$

where ℓ_{C_1} and ℓ_{C_2} are both negative quantities. The rotation matrices needed for vector transformation from one frame to another are

$$\boldsymbol{R}_i^{i-1} = \begin{bmatrix} c_i & -s_i & 0 \\ s_i & c_i & 0 \\ 0 & 0 & 1 \end{bmatrix} \quad i = 1, 2 \qquad \boldsymbol{R}_3^2 = \boldsymbol{I}.$$

Further, it is assumed that the axes of rotation of the two rotors coincide with the respective joint axes, i.e., $\boldsymbol{z}_{m_i}^{i-1} = \boldsymbol{z}_0 = [\,0 \quad 0 \quad 1\,]^T$ for $i = 1, 2$.

According to (7.107)–(7.114), the Newton–Euler algorithm requires the execution of the following steps:

- Forward recursion: Link 1

$$\boldsymbol{\omega}_1^1 = \begin{bmatrix} 0 \\ 0 \\ \dot{\vartheta}_1 \end{bmatrix}$$

$$\dot{\boldsymbol{\omega}}_1^1 = \begin{bmatrix} 0 \\ 0 \\ \ddot{\vartheta}_1 \end{bmatrix}$$

$$\ddot{\boldsymbol{p}}_1^1 = \begin{bmatrix} -a_1\dot{\vartheta}_1^2 + gs_1 \\ a_1\ddot{\vartheta}_1 + gc_1 \\ 0 \end{bmatrix}$$

$$\ddot{\boldsymbol{p}}_{C_1}^1 = \begin{bmatrix} -(\ell_{C_1} + a_1)\dot{\vartheta}_1^2 + gs_1 \\ (\ell_{C_1} + a_1)\ddot{\vartheta}_1 + gc_1 \\ 0 \end{bmatrix}$$

$$\dot{\boldsymbol{\omega}}_{m_1}^0 = \begin{bmatrix} 0 \\ 0 \\ k_{r1}\ddot{\vartheta}_1 \end{bmatrix}.$$

- Forward recursion: Link 2

$$\boldsymbol{\omega}_2^2 = \begin{bmatrix} 0 \\ 0 \\ \dot{\vartheta}_1 + \dot{\vartheta}_2 \end{bmatrix}$$

$$\dot{\boldsymbol{\omega}}_2^2 = \begin{bmatrix} 0 \\ 0 \\ \ddot{\vartheta}_1 + \ddot{\vartheta}_2 \end{bmatrix}$$

$$\ddot{\boldsymbol{p}}_2^2 = \begin{bmatrix} a_1 s_2\ddot{\vartheta}_1 - a_1 c_2\dot{\vartheta}_1^2 - a_2(\dot{\vartheta}_1 + \dot{\vartheta}_2)^2 + gs_{12} \\ a_1 c_2\ddot{\vartheta}_1 + a_2(\ddot{\vartheta}_1 + \ddot{\vartheta}_2) + a_1 s_2\dot{\vartheta}_1^2 + gc_{12} \\ 0 \end{bmatrix}$$

$$\ddot{\boldsymbol{p}}_{C_2}^2 = \begin{bmatrix} a_1 s_2\ddot{\vartheta}_1 - a_1 c_2\dot{\vartheta}_1^2 - (\ell_{C_2} + a_2)(\dot{\vartheta}_1 + \dot{\vartheta}_2)^2 + gs_{12} \\ a_1 c_2\ddot{\vartheta}_1 + (\ell_{C_2} + a_2)(\ddot{\vartheta}_1 + \ddot{\vartheta}_2) + a_1 s_2\dot{\vartheta}_1^2 + gc_{12} \\ 0 \end{bmatrix}$$

$$\dot{\boldsymbol{\omega}}_{m_2}^1 = \begin{bmatrix} 0 \\ 0 \\ \ddot{\vartheta}_1 + k_{r2}\ddot{\vartheta}_2 \end{bmatrix}.$$

- Backward recursion: Link 2

$$\boldsymbol{f}_2^2 = \begin{bmatrix} m_2\big(a_1 s_2 \ddot{\vartheta}_1 - a_1 c_2 \dot{\vartheta}_1^2 - (\ell_{C_2} + a_2)(\dot{\vartheta}_1 + \dot{\vartheta}_2)^2 + g s_{12}\big) \\ m_2\big(a_1 c_2 \ddot{\vartheta}_1 + (\ell_{C_2} + a_2)(\ddot{\vartheta}_1 + \ddot{\vartheta}_2) + a_1 s_2 \dot{\vartheta}_1^2 + g c_{12}\big) \\ 0 \end{bmatrix}$$

$$\boldsymbol{\mu}_2^2 = \begin{bmatrix} * \\ * \\ \bar{I}_{2zz}(\ddot{\vartheta}_1 + \ddot{\vartheta}_2) + m_2(\ell_{C_2} + a_2)^2(\ddot{\vartheta}_1 + \ddot{\vartheta}_2) + m_2 a_1(\ell_{C_2} + a_2) c_2 \ddot{\vartheta}_1 \\ \qquad + m_2 a_1(\ell_{C_2} + a_2) s_2 \dot{\vartheta}_1^2 + m_2(\ell_{C_2} + a_2) g c_{12} \end{bmatrix}$$

$$\begin{aligned} \tau_2 = {} & \big(\bar{I}_{2zz} + m_2\left((\ell_{C_2} + a_2)^2 + a_1(\ell_{C_2} + a_2)c_2\right) + k_{r2} I_{m_2}\big)\ddot{\vartheta}_1 \\ & + \left(\bar{I}_{2zz} + m_2(\ell_{C_2} + a_2)^2 + k_{r2}^2 I_{m_2}\right)\ddot{\vartheta}_2 \\ & + m_2 a_1(\ell_{C_2} + a_2) s_2 \dot{\vartheta}_1^2 + m_2(\ell_{C_2} + a_2) g c_{12}. \end{aligned}$$

- Backward recursion: Link 1

$$\boldsymbol{f}_1^1 = \begin{bmatrix} -m_2(\ell_{C_2} + a_2) s_2(\ddot{\vartheta}_1 + \ddot{\vartheta}_2) - m_1(\ell_{C_1} + a_1)\dot{\vartheta}_1^2 - m_2 a_1 \dot{\vartheta}_1^2 \\ -m_2(\ell_{C_2} + a_2) c_2(\dot{\vartheta}_1 + \dot{\vartheta}_2)^2 + (m_1 + m_2) g s_1 \\ m_1(\ell_{C_1} + a_1)\ddot{\vartheta}_1 + m_2 a_1 \ddot{\vartheta}_1 + m_2(\ell_{C_2} + a_2) c_2(\ddot{\vartheta}_1 + \ddot{\vartheta}_2) \\ -m_2(\ell_{C_2} + a_2) s_2(\dot{\vartheta}_1 + \dot{\vartheta}_2)^2 + (m_1 + m_2) g c_1 \\ 0 \end{bmatrix}$$

$$\boldsymbol{\mu}_1^1 = \begin{bmatrix} * \\ * \\ \bar{I}_{1zz}\ddot{\vartheta}_1 + m_2 a_1^2 \ddot{\vartheta}_1 + m_1(\ell_{C_1} + a_1)^2 \ddot{\vartheta}_1 + m_2 a_1(\ell_{C_2} + a_2) c_2 \ddot{\vartheta}_1 \\ \qquad + \bar{I}_{2zz}(\ddot{\vartheta}_1 + \ddot{\vartheta}_2) + m_2 a_1(\ell_{C_2} + a_2) c_2(\ddot{\vartheta}_1 + \ddot{\vartheta}_2) \\ \qquad + m_2(\ell_{C_2} + a_2)^2(\ddot{\vartheta}_1 + \ddot{\vartheta}_2) + k_{r2} I_{m_2} \ddot{\vartheta}_2 \\ \qquad + m_2 a_1(\ell_{C_2} + a_2) s_2 \dot{\vartheta}_1^2 - m_2 a_1(\ell_{C_2} + a_2) s_2(\dot{\vartheta}_1 + \dot{\vartheta}_2)^2 \\ \qquad + m_1(\ell_{C_1} + a_1) g c_1 + m_2 a_1 g c_1 + m_2(\ell_{C_2} + a_2) g c_{12} \end{bmatrix}$$

$$\begin{aligned} \tau_1 = {} & \Big(\bar{I}_{1zz} + m_1(\ell_{C_1} + a_1)^2 + k_{r1}^2 I_{m_1} + \bar{I}_{2zz} \\ & \qquad + m_2\left(a_1^2 + (\ell_{C_2} + a_2)^2 + 2a_1(\ell_{C_2} + a_2)c_2\right)\Big)\ddot{\vartheta}_1 \\ & + \Big(\bar{I}_{2zz} + m_2\left((\ell_{C_2} + a_2)^2 + a_1(\ell_{C_2} + a_2)c_2\right) + k_{r2} I_{m_2}\Big)\ddot{\vartheta}_2 \\ & - 2m_2 a_1(\ell_{C_2} + a_2) s_2 \dot{\vartheta}_1 \dot{\vartheta}_2 - m_2 a_1(\ell_{C_2} + a_2) s_2 \dot{\vartheta}_2^2 \\ & + \big(m_1(\ell_{C_1} + a_1) + m_2 a_1\big) g c_1 + m_2(\ell_{C_2} + a_2) g c_{12}. \end{aligned}$$

As for the moment components, those marked by the symbol '$*$' have not been computed, since they are not related to the joint torques τ_2 and τ_1.

Expressing the dynamic parameters in the above torques as a function of the link and rotor parameters as in (7.83) yields

$$\begin{aligned} m_1 &= m_{\ell_1} + m_{m_2} \\ m_1 \ell_{C_1} &= m_{\ell_1}(\ell_1 - a_1) \\ \bar{I}_{1zz} + m_1 \ell_{C_1}^2 = \widehat{I}_1 &= I_{\ell_1} + m_{\ell_1}(\ell_1 - a_1)^2 + I_{m_2} \\ m_2 &= m_{\ell_2} \\ m_2 \ell_{C_2} &= m_{\ell_2}(\ell_2 - a_2) \\ \bar{I}_{2zz} + m_2 \ell_{C_2}^2 = \widehat{I}_2 &= I_{\ell_2} + m_{\ell_2}(\ell_2 - a_2)^2. \end{aligned}$$

On the basis of these relations, it can be verified that the resulting dynamic model coincides with the model derived in (7.82) with Lagrange formulation.

7.6 Direct Dynamics and Inverse Dynamics

Both Lagrange formulation and Newton–Euler formulation allow the computation of the relationship between the joint torques — and, if present, the end-effector forces — and the motion of the structure. A comparison between the two approaches reveals what follows. The *Lagrange* formulation has the following advantages:

- It is *systematic* and of immediate comprehension.
- It provides the equations of motion in a compact *analytical form* containing the inertia matrix, the matrix in the centrifugal and Coriolis forces, and the vector of gravitational forces. Such a form is advantageous for *control design*.
- It is effective if it is wished to include more complex mechanical effects such as flexible link deformation.

The *Newton–Euler* formulation has the following fundamental advantage:

- It is an inherently *recursive* method that is computationally efficient.

In the study of dynamics, it is relevant to find a solution to two kinds of problems concerning computation of direct dynamics and inverse dynamics.

The *direct dynamics* problem consists of determining, for $t > t_0$, the joint accelerations $\ddot{\boldsymbol{q}}(t)$ (and thus $\dot{\boldsymbol{q}}(t)$, $\boldsymbol{q}(t)$) resulting from the given joint torques $\boldsymbol{\tau}(t)$ — and the possible end-effector forces $\boldsymbol{h}_e(t)$ — once the initial positions $\boldsymbol{q}(t_0)$ and velocities $\dot{\boldsymbol{q}}(t_0)$ are known (initial state of the system).

The *inverse dynamics* problem consists of determining the joint torques $\boldsymbol{\tau}(t)$ which are needed to generate the motion specified by the joint accelerations $\ddot{\boldsymbol{q}}(t)$, velocities $\dot{\boldsymbol{q}}(t)$, and positions $\boldsymbol{q}(t)$ — once the possible end-effector forces $\boldsymbol{h}_e(t)$ are known.

Solving the direct dynamics problem is useful for manipulator *simulation*. Direct dynamics allows the motion of the real physical system to be described in terms of the joint accelerations, when a set of assigned joint torques is applied to the manipulator; joint velocities and positions can be obtained by integrating the system of nonlinear differential equations.

Since the equations of motion obtained with Lagrange formulation give the analytical relationship between the joint torques (and the end-effector forces) and the joint positions, velocities and accelerations, these can be computed from (7.42) as

$$\ddot{\boldsymbol{q}} = \boldsymbol{B}^{-1}(\boldsymbol{q})(\boldsymbol{\tau} - \boldsymbol{\tau}') \tag{7.115}$$

where

$$\boldsymbol{\tau}'(\boldsymbol{q}, \dot{\boldsymbol{q}}) = \boldsymbol{C}(\boldsymbol{q}, \dot{\boldsymbol{q}})\dot{\boldsymbol{q}} + \boldsymbol{F}_v\dot{\boldsymbol{q}} + \boldsymbol{F}_s\,\mathbf{sgn}\,(\dot{\boldsymbol{q}}) + \boldsymbol{g}(\boldsymbol{q}) + \boldsymbol{J}^T(\boldsymbol{q})\boldsymbol{h}_e \tag{7.116}$$

denotes the torque contributions depending on joint positions and velocities. Therefore, for simulation of manipulator motion, once the state at the time instant t_k is known in terms of the position $\boldsymbol{q}(t_k)$ and velocity $\dot{\boldsymbol{q}}(t_k)$, the acceleration $\ddot{\boldsymbol{q}}(t_k)$ can be computed by (7.115). Then using a numerical integration method, e.g., Runge–Kutta, with integration step Δt, the velocity $\dot{\boldsymbol{q}}(t_{k+1})$ and position $\boldsymbol{q}(t_{k+1})$ at the instant $t_{k+1} = t_k + \Delta t$ can be computed.

If the equations of motion are obtained with Newton–Euler formulation, it is possible to compute direct dynamics by using a computationally more efficient method. In fact, for given $\boldsymbol{q}$ and $\dot{\boldsymbol{q}}$, the torques $\boldsymbol{\tau}'(\boldsymbol{q}, \dot{\boldsymbol{q}})$ in (7.116) can be computed as the torques given by the algorithm of Fig. 7.14 with $\ddot{\boldsymbol{q}} = \boldsymbol{0}$. Further, column $\boldsymbol{b}_i$ of matrix $\boldsymbol{B}(\boldsymbol{q})$ can be computed as the torque vector given by the algorithm of Fig. 7.14 with $\boldsymbol{g}_0 = \boldsymbol{0}$, $\dot{\boldsymbol{q}} = \boldsymbol{0}$, $\ddot{q}_i = 1$ and $\ddot{q}_j = 0$ for $j \neq i$; iterating this procedure for $i = 1, \ldots, n$ leads to constructing the matrix $\boldsymbol{B}(\boldsymbol{q})$. Hence, from the current values of $\boldsymbol{B}(\boldsymbol{q})$ and $\boldsymbol{\tau}'(\boldsymbol{q}, \dot{\boldsymbol{q}})$, and the given $\boldsymbol{\tau}$, the equations in (7.115) can be integrated as illustrated above.

Solving the inverse dynamics problem is useful for manipulator trajectory planning and control algorithm implementation. Once a joint trajectory is specified in terms of positions, velocities and accelerations (typically as a result of an inverse kinematics procedure), and if the end-effector forces are known, inverse dynamics allows computation of the torques to be applied to the joints to obtain the desired motion. This computation turns out to be useful both for verifying feasibility of the imposed trajectory and for compensating nonlinear terms in the dynamic model of a manipulator. To this end, Newton–Euler formulation provides a computationally efficient recursive method for on-line computation of inverse dynamics. Nevertheless, it can be shown that also Lagrange formulation is liable to a computationally efficient recursive implementation, though with a nonnegligible reformulation effort.

For an n-joint manipulator the *number of operations* required is:[8]

[8] See Sect. E.1 for the definition of computational complexity of an algorithm.

- $O(n^2)$ for computing *direct dynamics*,
- $O(n)$ for computing *inverse dynamics*.

7.7 Dynamic Scaling of Trajectories

The existence of *dynamic constraints* to be taken into account for trajectory generation has been mentioned in Sect. 4.1. In practice, with reference to the given trajectory time or path shape (segments with high curvature), the trajectories that can be obtained with any of the previously illustrated methods may impose too severe dynamic performance for the manipulator. A typical case is that when the required torques to generate the motion are larger than the maximum torques the actuators can supply. In this case, an infeasible trajectory has to be suitably time-scaled.

Suppose a trajectory has been generated for all the manipulator joints as $\boldsymbol{q}(t)$, for $t \in [0, t_f]$. Computing inverse dynamics allows the evaluation of the time history of the torques $\boldsymbol{\tau}(t)$ required for the execution of the given motion. By comparing the obtained torques with the *torque limits* available at the actuators, it is easy to check whether or not the trajectory is actually executable. The problem is then to seek an automatic trajectory *dynamic scaling* technique — avoiding inverse dynamics recomputation — so that the manipulator can execute the motion on the specified path with a proper timing law without exceeding the torque limits.

Consider the manipulator dynamic model as given in (7.42) with $\boldsymbol{F}_v = \boldsymbol{O}$, $\boldsymbol{F}_s = \boldsymbol{O}$ and $\boldsymbol{h}_e = \boldsymbol{0}$, for simplicity. The term $\boldsymbol{C}(\boldsymbol{q}, \dot{\boldsymbol{q}})$ accounting for centrifugal and Coriolis forces has a quadratic dependence on joint velocities, and thus it can be formally rewritten as

$$\boldsymbol{C}(\boldsymbol{q}, \dot{\boldsymbol{q}})\dot{\boldsymbol{q}} = \boldsymbol{\Gamma}(\boldsymbol{q})[\dot{\boldsymbol{q}}\dot{\boldsymbol{q}}], \tag{7.117}$$

where $[\dot{\boldsymbol{q}}\dot{\boldsymbol{q}}]$ indicates the symbolic notation of the $(n(n+1)/2 \times 1)$ vector

$$[\dot{\boldsymbol{q}}\dot{\boldsymbol{q}}] = [\, \dot{q}_1^2 \quad \dot{q}_1\dot{q}_2 \quad \dots \quad \dot{q}_{n-1}\dot{q}_n \quad \dot{q}_n^2 \,]^T;$$

$\boldsymbol{\Gamma}(\boldsymbol{q})$ is a proper $(n \times n(n+1)/2)$ matrix that satisfies (7.117). In view of such position, the manipulator dynamic model can be expressed as

$$\boldsymbol{B}(\boldsymbol{q}(t))\ddot{\boldsymbol{q}}(t) + \boldsymbol{\Gamma}(\boldsymbol{q}(t))[\dot{\boldsymbol{q}}(t)\dot{\boldsymbol{q}}(t)] + \boldsymbol{g}(\boldsymbol{q}(t)) = \boldsymbol{\tau}(t), \tag{7.118}$$

where the explicit dependence on time t has been shown.

Consider the new variable $\bar{\boldsymbol{q}}(r(t))$ satisfying the equation

$$\boldsymbol{q}(t) = \bar{\boldsymbol{q}}(r(t)), \tag{7.119}$$

where $r(t)$ is a strictly increasing scalar function of time with $r(0) = 0$ and $r(t_f) = \bar{t}_f$.

Differentiating (7.119) twice with respect to time provides the following relations:

$$\dot{\boldsymbol{q}} = \dot{r}\bar{\boldsymbol{q}}'(r) \tag{7.120}$$

$$\ddot{\boldsymbol{q}} = \dot{r}^2\bar{\boldsymbol{q}}''(r) + \ddot{r}\bar{\boldsymbol{q}}'(r) \tag{7.121}$$

where the prime denotes the derivative with respect to r. Substituting (7.120), (7.121) into (7.118) yields

$$\dot{r}^2\Big(\boldsymbol{B}(\bar{\boldsymbol{q}}(r))\bar{\boldsymbol{q}}''(r) + \boldsymbol{\Gamma}(\bar{\boldsymbol{q}}(r))[\bar{\boldsymbol{q}}'(r)\bar{\boldsymbol{q}}'(r)]\Big) + \ddot{r}\boldsymbol{B}(\bar{\boldsymbol{q}}(r))\bar{\boldsymbol{q}}'(r) + \boldsymbol{g}(\bar{\boldsymbol{q}}(r)) = \boldsymbol{\tau}. \tag{7.122}$$

In (7.118) it is possible to identify the term

$$\boldsymbol{\tau}_s(t) = \boldsymbol{B}(\boldsymbol{q}(t))\ddot{\boldsymbol{q}}(t) + \boldsymbol{\Gamma}(\boldsymbol{q}(t))[\dot{\boldsymbol{q}}(t)\dot{\boldsymbol{q}}(t)], \tag{7.123}$$

representing the torque contribution that depends on velocities and accelerations. Correspondingly, in (7.122) one can set

$$\boldsymbol{\tau}_s(t) = \dot{r}^2\Big(\boldsymbol{B}(\bar{\boldsymbol{q}}(r))\bar{\boldsymbol{q}}''(r) + \boldsymbol{\Gamma}(\bar{\boldsymbol{q}}(r))[\bar{\boldsymbol{q}}'(r)\bar{\boldsymbol{q}}'(r)]\Big) + \ddot{r}\boldsymbol{B}(\bar{\boldsymbol{q}}(r))\bar{\boldsymbol{q}}'(r). \tag{7.124}$$

By analogy with (7.123), it can be written

$$\bar{\boldsymbol{\tau}}_s(r) = \boldsymbol{B}(\bar{\boldsymbol{q}}(r))\bar{\boldsymbol{q}}''(r) + \boldsymbol{\Gamma}(\bar{\boldsymbol{q}}(r))[\bar{\boldsymbol{q}}'(r)\bar{\boldsymbol{q}}'(r)] \tag{7.125}$$

and then (7.124) becomes

$$\boldsymbol{\tau}_s(t) = \dot{r}^2\bar{\boldsymbol{\tau}}_s(r) + \ddot{r}\boldsymbol{B}(\bar{\boldsymbol{q}}(r))\bar{\boldsymbol{q}}'(r). \tag{7.126}$$

The expression in (7.126) gives the relationship between the torque contributions depending on velocities and accelerations required by the manipulator when this is subject to motions having the same path but different timing laws, obtained through a time scaling of joint variables as in (7.119).

Gravitational torques have not been considered, since they are a function of the joint positions only, and thus their contribution is not influenced by time scaling.

The simplest choice for the scaling function $r(t)$ is certainly the *linear* function

$$r(t) = ct$$

with c a positive constant. In this case, (7.126) becomes

$$\boldsymbol{\tau}_s(t) = c^2\bar{\boldsymbol{\tau}}_s(ct),$$

which reveals that a linear time scaling by c causes a scaling of the magnitude of the torques by the coefficient c^2. Let $c > 1$: (7.119) shows that the trajectory described by $\bar{\boldsymbol{q}}(r(t))$, assuming $r = ct$ as the independent variable, has a duration $\bar{t}_f > t_f$ to cover the entire path specified by $\boldsymbol{q}$. Correspondingly, the

torque contributions $\bar{\boldsymbol{\tau}}_s(ct)$ computed as in (7.125) are scaled by the factor c^2 with respect to the torque contributions $\boldsymbol{\tau}_s(t)$ required to execute the original trajectory $\boldsymbol{q}(t)$.

With the use of a recursive algorithm for inverse dynamics computation, it is possible to check whether the torques exceed the allowed limits during trajectory execution; obviously, limit violation should not be caused by the sole gravity torques. It is necessary to find the joint for which the torque has exceeded the limit more than the others, and to compute the torque contribution subject to scaling, which in turn determines the factor c^2. It is then possible to compute the time-scaled trajectory as a function of the new time variable $r = ct$ which no longer exceeds torque limits. It should be pointed out, however, that with this kind of linear scaling the entire trajectory may be penalized, even when a torque limit on a single joint is exceeded only for a short interval of time.

7.8 Operational Space Dynamic Model

As an alternative to the joint space dynamic model, the equations of motion of the system can be expressed directly in the operational space; to this end it is necessary to find a *dynamic model* which describes the relationship between the generalized forces acting on the manipulator and the number of minimal variables chosen to describe the end-effector position and orientation in the *operational space*.

Similar to kinematic description of a manipulator in the operational space, the presence of redundant DOFs and/or kinematic and representation singularities deserves careful attention in the derivation of an operational space dynamic model.

The determination of the dynamic model with Lagrange formulation using operational space variables allows a complete description of the system motion only in the case of a *nonredundant* manipulator, when the above variables constitute a set of *generalized coordinates* in terms of which the kinetic energy, the potential energy, and the nonconservative forces doing work on them can be expressed.

This way of proceeding does not provide a complete description of dynamics for a *redundant* manipulator; in this case, in fact, it is reasonable to expect the occurrence of *internal motions* of the structure caused by those joint generalized forces which do not affect the end-effector motion.

To develop an operational space model which can be adopted for both redundant and nonredundant manipulators, it is then convenient to start from the joint space model which is in all general. In fact, solving (7.42) for the joint accelerations, and neglecting the joint friction torques for simplicity, yields

$$\ddot{\boldsymbol{q}} = -\boldsymbol{B}^{-1}(\boldsymbol{q})\boldsymbol{C}(\boldsymbol{q},\dot{\boldsymbol{q}})\dot{\boldsymbol{q}} - \boldsymbol{B}^{-1}(\boldsymbol{q})\boldsymbol{g}(\boldsymbol{q}) + \boldsymbol{B}^{-1}(\boldsymbol{q})\boldsymbol{J}^T(\boldsymbol{q})(\boldsymbol{\gamma}_e - \boldsymbol{h}_e), \quad (7.127)$$

where the joint torques $\boldsymbol{\tau}$ have been expressed in terms of the equivalent end-effector forces $\boldsymbol{\gamma}$ according to (3.111). It is worth noting that $\boldsymbol{h}$ represents the contribution of the end-effector forces due to contact with the environment, whereas $\boldsymbol{\gamma}$ expresses the contribution of the end-effector forces due to joint actuation.

On the other hand, the second-order differential kinematics equation in (3.98) describes the relationship between joint space and operational space accelerations, i.e.,

$$\ddot{\boldsymbol{x}}_e = \boldsymbol{J}_A(\boldsymbol{q})\ddot{\boldsymbol{q}} + \dot{\boldsymbol{J}}_A(\boldsymbol{q}, \dot{\boldsymbol{q}})\dot{\boldsymbol{q}}.$$

The solution in (7.127) features the geometric Jacobian $\boldsymbol{J}$, whereas the analytical Jacobian $\boldsymbol{J}_A$ appears in (3.98). For notation uniformity, in view of (3.66), one can set

$$\boldsymbol{T}_A^T(\boldsymbol{x}_e)\boldsymbol{\gamma}_e = \boldsymbol{\gamma}_A \qquad \boldsymbol{T}_A^T(\boldsymbol{x}_e)\boldsymbol{h}_e = \boldsymbol{h}_A \tag{7.128}$$

where $\boldsymbol{T}_A$ is the transformation matrix between the two Jacobians. Substituting (7.127) into (3.98) and accounting for (7.128) gives

$$\ddot{\boldsymbol{x}}_e = -\boldsymbol{J}_A\boldsymbol{B}^{-1}\boldsymbol{C}\dot{\boldsymbol{q}} - \boldsymbol{J}_A\boldsymbol{B}^{-1}\boldsymbol{g} + \dot{\boldsymbol{J}}_A\dot{\boldsymbol{q}} + \boldsymbol{J}_A\boldsymbol{B}^{-1}\boldsymbol{J}_A^T(\boldsymbol{\gamma}_A - \boldsymbol{h}_A). \tag{7.129}$$

where the dependence on $\boldsymbol{q}$ and $\dot{\boldsymbol{q}}$ has been omitted. With the positions

$$\boldsymbol{B}_A = (\boldsymbol{J}_A\boldsymbol{B}^{-1}\boldsymbol{J}_A^T)^{-1} \tag{7.130}$$

$$\boldsymbol{C}_A\dot{\boldsymbol{x}}_e = \boldsymbol{B}_A\boldsymbol{J}_A\boldsymbol{B}^{-1}\boldsymbol{C}\dot{\boldsymbol{q}} - \boldsymbol{B}_A\dot{\boldsymbol{J}}_A\dot{\boldsymbol{q}} \tag{7.131}$$

$$\boldsymbol{g}_A = \boldsymbol{B}_A\boldsymbol{J}_A\boldsymbol{B}^{-1}\boldsymbol{g}, \tag{7.132}$$

the expression in (7.129) can be rewritten as

$$\boldsymbol{B}_A(\boldsymbol{x}_e)\ddot{\boldsymbol{x}}_e + \boldsymbol{C}_A(\boldsymbol{x}_e, \dot{\boldsymbol{x}}_e)\dot{\boldsymbol{x}}_e + \boldsymbol{g}_A(\boldsymbol{x}_e) = \boldsymbol{\gamma}_A - \boldsymbol{h}_A, \tag{7.133}$$

which is formally analogous to the joint space dynamic model (7.42). Notice that the matrix $\boldsymbol{J}_A\boldsymbol{B}^{-1}\boldsymbol{J}_A^T$ is invertible if and only if $\boldsymbol{J}_A$ is full-rank, that is, in the absence of both kinematic and representation singularities.

For a nonredundant manipulator in a nonsingular configuration, the expressions in (7.130)–(7.132) become:

$$\boldsymbol{B}_A = \boldsymbol{J}_A^{-T}\boldsymbol{B}\boldsymbol{J}_A^{-1} \tag{7.134}$$

$$\boldsymbol{C}_A\dot{\boldsymbol{x}}_e = \boldsymbol{J}_A^{-T}\boldsymbol{C}\dot{\boldsymbol{q}} - \boldsymbol{B}_A\dot{\boldsymbol{J}}_A\dot{\boldsymbol{q}} \tag{7.135}$$

$$\boldsymbol{g}_A = \boldsymbol{J}_A^{-T}\boldsymbol{g}. \tag{7.136}$$

As anticipated above, the main feature of the obtained model is its formal validity also for a redundant manipulator, even though the variables $\boldsymbol{x}_e$ do not constitute a set of generalized coordinates for the system; in this case, the matrix $\boldsymbol{B}_A$ is representative of a *kinetic pseudo-energy*.

In the following, the utility of the operational space dynamic model in (7.133) for solving direct and inverse dynamics problems is investigated. The

following derivation is meaningful for redundant manipulators; for a nonredundant manipulator, in fact, using (7.133) does not pose specific problems as long as $\boldsymbol{J}_A$ is nonsingular ((7.134)–(7.136)).

With reference to operational space, the *direct dynamics* problem consists of determining the resulting end-effector accelerations $\ddot{\boldsymbol{x}}_e(t)$ (and thus $\dot{\boldsymbol{x}}_e(t)$, $\boldsymbol{x}_e(t)$) from the given joint torques $\boldsymbol{\tau}(t)$ and end-effector forces $\boldsymbol{h}_e(t)$. For a redundant manipulator, (7.133) cannot be directly used, since (3.111) has a solution in $\boldsymbol{\gamma}_e$ only if $\boldsymbol{\tau} \in \mathcal{R}(\boldsymbol{J}^T)$. It follows that for simulation purposes, the solution to the problem is naturally obtained in the joint space; in fact, the expression in (7.42) allows the computation of $\boldsymbol{q}$, $\dot{\boldsymbol{q}}$, $\ddot{\boldsymbol{q}}$ which, substituted into the direct kinematics equations in ((2.82), (3.62), (3.98), give $\boldsymbol{x}_e$, $\dot{\boldsymbol{x}}_e$, $\ddot{\boldsymbol{x}}_e$, respectively.

Formulation of an *inverse dynamics* problem in the operational space requires the determination of the joint torques $\boldsymbol{\tau}(t)$ that are needed to generate a specific motion assigned in terms of $\ddot{\boldsymbol{x}}_e(t)$, $\dot{\boldsymbol{x}}_e(t)$, $\boldsymbol{x}_e(t)$, for given end-effector forces $\boldsymbol{h}_e(t)$. A possible way of solution is to solve a complete inverse kinematics problem for (2.82), (3.62), (3.98), and then compute the required torques with the joint space inverse dynamics as in (7.42). Hence, for redundant manipulators, redundancy resolution is performed at kinematic level.

An alternative solution to the inverse dynamics problem consists of computing $\boldsymbol{\gamma}_A$ as in (7.133) and the joint torques $\boldsymbol{\tau}$ as in (3.111). In this way, however, the presence of redundant DOFs is not exploited at all, since the computed torques do not generate internal motions of the structure.

If it is desired to find a formal solution that allows redundancy resolution at dynamic level, it is necessary to determine those torques corresponding to the equivalent end-effector forces computed as in (7.133). By analogy with the differential kinematics solution (3.54), the expression of the torques to be determined will feature the presence of a minimum-norm term and a homogeneous term. Since the joint torques have to be computed, it is convenient to express the model (7.133) in terms of $\boldsymbol{q}$, $\dot{\boldsymbol{q}}$, $\ddot{\boldsymbol{q}}$. By recalling the positions (7.131), (7.132), the expression in (7.133) becomes

$$\boldsymbol{B}_A(\ddot{\boldsymbol{x}}_e - \dot{\boldsymbol{J}}_A\dot{\boldsymbol{q}}) + \boldsymbol{B}_A\boldsymbol{J}_A\boldsymbol{B}^{-1}\boldsymbol{C}\dot{\boldsymbol{q}} + \boldsymbol{B}_A\boldsymbol{J}_A\boldsymbol{B}^{-1}\boldsymbol{g} = \boldsymbol{\gamma}_A - \boldsymbol{h}_A$$

and, in view of (3.98),

$$\boldsymbol{B}_A\boldsymbol{J}_A\ddot{\boldsymbol{q}} + \boldsymbol{B}_A\boldsymbol{J}_A\boldsymbol{B}^{-1}\boldsymbol{C}\dot{\boldsymbol{q}} + \boldsymbol{B}_A\boldsymbol{J}_A\boldsymbol{B}^{-1}\boldsymbol{g} = \boldsymbol{\gamma}_A - \boldsymbol{h}_A. \tag{7.137}$$

By setting

$$\bar{\boldsymbol{J}}_A(\boldsymbol{q}) = \boldsymbol{B}^{-1}(\boldsymbol{q})\boldsymbol{J}_A^T(\boldsymbol{q})\boldsymbol{B}_A(\boldsymbol{q}), \tag{7.138}$$

the expression in (7.137) becomes

$$\bar{\boldsymbol{J}}_A^T(\boldsymbol{B}\ddot{\boldsymbol{q}} + \boldsymbol{C}\dot{\boldsymbol{q}} + \boldsymbol{g}) = \boldsymbol{\gamma}_A - \boldsymbol{h}_A. \tag{7.139}$$

At this point, from the joint space dynamic model in (7.42), it is easy to recognize that (7.139) can be written as

$$\bar{\boldsymbol{J}}_A^T(\boldsymbol{\tau} - \boldsymbol{J}_A^T\boldsymbol{h}_A) = \boldsymbol{\gamma}_A - \boldsymbol{h}_A$$

from which

$$\bar{\boldsymbol{J}}_A^T \boldsymbol{\tau} = \boldsymbol{\gamma}_A. \tag{7.140}$$

The general solution to (7.140) is of the form (see Problem 7.11)

$$\boldsymbol{\tau} = \boldsymbol{J}_A^T(\boldsymbol{q})\boldsymbol{\gamma}_A + \big(\boldsymbol{I}_n - \boldsymbol{J}_A^T(\boldsymbol{q})\bar{\boldsymbol{J}}_A^T(\boldsymbol{q})\big)\boldsymbol{\tau}_0, \tag{7.141}$$

that can be derived by observing that $\boldsymbol{J}_A^T$ in (7.138) is a *right pseudo-inverse* of $\bar{\boldsymbol{J}}_A^T$ weighted by the inverse of the inertia matrix $\boldsymbol{B}^{-1}$. The $(n \times 1)$ vector of arbitrary torques $\boldsymbol{\tau}_0$ in (7.141) does not contribute to the end-effector forces, since it is projected in the null space of $\bar{\boldsymbol{J}}_A^T$.

To summarize, for given $\boldsymbol{x}_e$, $\dot{\boldsymbol{x}}_e$, $\ddot{\boldsymbol{x}}_e$ and $\boldsymbol{h}_A$, the expression in (7.133) allows the computation of $\boldsymbol{\gamma}_A$. Then, (7.141) gives the torques $\boldsymbol{\tau}$ which, besides executing the assigned end-effector motion, generate internal motions of the structure to be employed for handling redundancy at dynamic level through a suitable choice of $\boldsymbol{\tau}_0$.

7.9 Dynamic Manipulability Ellipsoid

The availability of the dynamic model allows formulation of the *dynamic manipulability ellipsoid* which provides a useful tool for manipulator dynamic performance analysis. This can be used for mechanical structure design as well as for seeking optimal manipulator configurations.

Consider the set of joint torques of constant (unit) norm

$$\boldsymbol{\tau}^T \boldsymbol{\tau} = 1 \tag{7.142}$$

describing the points on the surface of a sphere. It is desired to describe the operational space accelerations that can be generated by the given set of joint torques.

For studying dynamic manipulability, suppose to consider the case of a manipulator standing still ($\dot{\boldsymbol{q}} = \boldsymbol{0}$), not in contact with the environment ($\boldsymbol{h}_e = \boldsymbol{0}$). The simplified model is

$$\boldsymbol{B}(\boldsymbol{q})\ddot{\boldsymbol{q}} + \boldsymbol{g}(\boldsymbol{q}) = \boldsymbol{\tau}. \tag{7.143}$$

The joint accelerations $\ddot{\boldsymbol{q}}$ can be computed from the second-order differential kinematics that can be obtained by differentiating (3.39), and imposing successively $\dot{\boldsymbol{q}} = \boldsymbol{0}$, leading to

$$\dot{\boldsymbol{v}}_e = \boldsymbol{J}(\boldsymbol{q})\ddot{\boldsymbol{q}}. \tag{7.144}$$

Solving for minimum-norm accelerations only, for a *nonsingular Jacobian*, and substituting in (7.143) yields the expression of the torques

$$\boldsymbol{\tau} = \boldsymbol{B}(\boldsymbol{q})\boldsymbol{J}^{\dagger}(\boldsymbol{q})\dot{\boldsymbol{v}}_e + \boldsymbol{g}(\boldsymbol{q}) \tag{7.145}$$

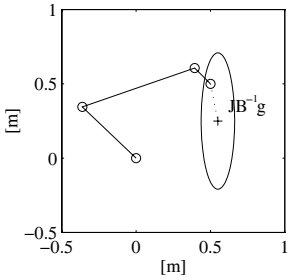

Fig. 7.15. Effect of gravity on the dynamic manipulability ellipsoid for a three-link planar arm

needed to derive the ellipsoid. In fact, substituting (7.145) into (7.142) gives

$$\big(\boldsymbol{B}(\boldsymbol{q})\boldsymbol{J}^{\dagger}(\boldsymbol{q})\dot{\boldsymbol{v}}_e + \boldsymbol{g}(\boldsymbol{q})\big)^T \big(\boldsymbol{B}(\boldsymbol{q})\boldsymbol{J}^{\dagger}(\boldsymbol{q})\dot{\boldsymbol{v}}_e + \boldsymbol{g}(\boldsymbol{q})\big) = 1.$$

The vector on the right-hand side of (7.145) can be rewritten as

$$\begin{aligned} \boldsymbol{B}\boldsymbol{J}^{\dagger}\dot{\boldsymbol{v}}_e + \boldsymbol{g} &= \boldsymbol{B}(\boldsymbol{J}^{\dagger}\dot{\boldsymbol{v}}_e + \boldsymbol{B}^{-1}\boldsymbol{g}) \\ &= \boldsymbol{B}(\boldsymbol{J}^{\dagger}\dot{\boldsymbol{v}}_e + \boldsymbol{B}^{-1}\boldsymbol{g} + \boldsymbol{J}^{\dagger}\boldsymbol{J}\boldsymbol{B}^{-1}\boldsymbol{g} - \boldsymbol{J}^{\dagger}\boldsymbol{J}\boldsymbol{B}^{-1}\boldsymbol{g}) \\ &= \boldsymbol{B}\big(\boldsymbol{J}^{\dagger}\dot{\boldsymbol{v}}_e + \boldsymbol{J}^{\dagger}\boldsymbol{J}\boldsymbol{B}^{-1}\boldsymbol{g} + (\boldsymbol{I}_n - \boldsymbol{J}^{\dagger}\boldsymbol{J})\boldsymbol{B}^{-1}\boldsymbol{g}\big), \end{aligned} \tag{7.146}$$

where the dependence on $\boldsymbol{q}$ has been omitted. According to what was done for solving (7.144), one can neglect the contribution of the accelerations given by $\boldsymbol{B}^{-1}\boldsymbol{g}$ which are in the null space of $\boldsymbol{J}$ and then produce no end-effector acceleration. Hence, (7.146) becomes

$$\boldsymbol{B}\boldsymbol{J}^{\dagger}\dot{\boldsymbol{v}}_e + \boldsymbol{g} = \boldsymbol{B}\boldsymbol{J}^{\dagger}(\dot{\boldsymbol{v}}_e + \boldsymbol{J}\boldsymbol{B}^{-1}\boldsymbol{g}) \tag{7.147}$$

and the dynamic manipulability ellipsoid can be expressed in the form

$$(\dot{\boldsymbol{v}}_e + \boldsymbol{J}\boldsymbol{B}^{-1}\boldsymbol{g})^T\boldsymbol{J}^{\dagger T}\boldsymbol{B}^T\boldsymbol{B}\boldsymbol{J}^{\dagger}(\dot{\boldsymbol{v}}_e + \boldsymbol{J}\boldsymbol{B}^{-1}\boldsymbol{g}) = 1. \tag{7.148}$$

The core of the quadratic form $\boldsymbol{J}^{\dagger T}\boldsymbol{B}^T\boldsymbol{B}\boldsymbol{J}^{\dagger}$ depends on the geometrical and inertial characteristics of the manipulator and determines the volume and principal axes of the ellipsoid. The vector $-\boldsymbol{J}\boldsymbol{B}^{-1}\boldsymbol{g}$, describing the contribution of gravity, produces a constant translation of the centre of the ellipsoid (for each manipulator configuration) with respect to the origin of the reference frame; see the example in Fig. 7.15 for a three-link planar arm.

The meaning of the dynamic manipulability ellipsoid is conceptually similar to that of the ellipsoids considered with reference to kineto-statics duality. In fact, the distance of a point on the surface of the ellipsoid from the end-effector gives a measure of the accelerations which can be imposed to the end-effector along the given direction, with respect to the constraint (7.142). With reference to Fig. 7.15, it is worth noticing how the presence of gravity

acceleration allows the execution of larger accelerations downward, as natural to predict.

In the case of a nonredundant manipulator, the ellipsoid reduces to

$$(\dot{\boldsymbol{v}}_e + \boldsymbol{J}\boldsymbol{B}^{-1}\boldsymbol{g})^T \boldsymbol{J}^{-T}\boldsymbol{B}^T\boldsymbol{B}\boldsymbol{J}^{-1}(\dot{\boldsymbol{v}}_e + \boldsymbol{J}\boldsymbol{B}^{-1}\boldsymbol{g}) = 1. \tag{7.149}$$

Bibliography

The derivation of the dynamic model for rigid manipulators can be found in several classical robotics texts, such as [180, 10, 248, 53, 217, 111].

The first works on the computation of the dynamic model of open-chain manipulators based on the Lagrange formulation are [234, 19, 221, 236]. A computationally efficient formulation is presented in [96].

Dynamic model computation for robotic systems having a closed-chain or a tree kinematic structure can be found in [11, 144] and [112], respectively. Joint friction models are analyzed in [9].

The notable properties of the dynamic model deriving from the principle of energy conservation are underlined in [213], on the basis of the work in [119]. Algorithms to find the parameterization of the dynamic model in terms of a minimum number of parameters are considered in [115], which utilizes the results in [166]. Methods for symbolic computation of those parameters are presented in [85] for open kinematic chains and [110] for closed kinematic chains. Parameter identification methods based on least-squares techniques are given in [13].

The Newton–Euler formulation is proposed in [172], and a computationally efficient version for inverse dynamics can be found in [142]; an analogous formulation is employed for direct dynamics computation in [237]. The Lagrange and Newton–Euler formulations are compared by a computational viewpoint in [211], while they are utilized in [201] for dynamic model computation with inclusion of inertial and gyroscopic effects of actuators. Efficient algorithms for direct dynamics computation are given in [76, 77].

The trajectory dynamic scaling technique is presented in [97]. The operational space dynamic model is illustrated in [114] and the concept of weighted pseudo-inverse of the inertia matrix is introduced in [78]. The manipulability ellipsoids are analyzed in [246, 38].

Problems

7.1. Find the dynamic model of a two-link Cartesian arm in the case when the second joint axis forms an angle of $\pi/4$ with the first joint axis; compare the result with the model of the manipulator in Fig. 7.3.

7.2. For the two-link planar arm of Sect. 7.3.2, prove that with a different choice of the matrix $\boldsymbol{C}$, (7.49) holds true while (7.48) does not.

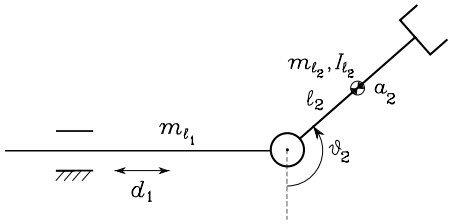

Fig. 7.16. Two-link planar arm with a prismatic joint and a revolute joint

7.3. Find the dynamic model of the SCARA manipulator in Fig. 2.36.

7.4. For the planar arm of Sect. 7.3.2, find a minimal parameterization of the dynamic model in (7.82).

7.5. Find the dynamic model of the two-link planar arm with a prismatic joint and a revolute joint in Fig. 7.16 with the Lagrange formulation. Then, consider the addition of a concentrated tip payload of mass m_L, and express the resulting model in a linear form with respect to a suitable set of dynamic parameters as in (7.81).

7.6. For the two-link planar arm of Fig. 7.4, find the dynamic model with the Lagrange formulation when the absolute angles with respect to the base frame are chosen as generalized coordinates. Discuss the result in view of a comparison with the model derived in (7.82).

7.7. Compute the joint torques for the two-link planar arm of Fig. 7.4 with the data and along the trajectories of Example 7.2, in the case of tip forces $\boldsymbol{f} = [\,500 \quad 500\,]^T$ N.

7.8. Find the dynamic model of the two-link planar arm with a prismatic joint and a revolute joint in Fig. 7.16 by using the recursive Newton–Euler algorithm.

7.9. For the two-link planar arm of Example 7.2, perform a computer implementation of the dynamic scaling technique with a linear scaling function for the trajectory of Fig. 7.5, assuming for the two joints the torque limit of 3000 N·m. Adopt a sampling time of 1 ms.

7.10. Show that for the operational space dynamic model (7.133) a skew-symmetry property holds which is analogous to (7.48).

7.11. Show how to obtain the general solution to (7.140) in the form (7.141).

7.12. For a nonredundant manipulator, compute the relationship between the dynamic manipulability measure that can be defined for the dynamic manipulability ellipsoid and the manipulability measure defined in (3.56).